Current Science
CS 5 (6), 5299-5337 (2025)
**Received 18 Oct** 2025 | **Accepted 30 October** 2025 | **Online Available 08 November** 2025
https://doi.org/10.52845/CS/2025-5-6-5

**Current Science**

Current Science

**OPEN ACCESS**

**ISSN (O) 2795-8639**

**Original Article**

# Identification Of Disulfidptosis-Related Genes In Glioblastoma Combining Bioinformatics Techniques And Machine Learning

**Daikang Xu[1,1], Guangyu Du[1,1], Jingxian Sun[1,1], Xiaolei Lan[1,2], Zhiyong Yan[1,2], Jianpeng Wang[1]***

**[1]Department of Neurosurgery,The Affiliated Hospital of Qingdao University,Qingdao,Shandong 266000, China**

***Corresponding Author: Jianpeng Wang**

**Abstract:**
Glioblastoma (GBM) is the most malignant brain tumor, and with high heterogeneity and subsequent temozolomide (TMZ) resistance, the traditional treatment are often suboptimal. Disulfidptosis, a newly proposed form of cell death, plays a crucial role in the progression of various tumors, and its involvement in glioblastoma (GBM) remains further exploration. In this study, we combined bioinformatics with multiple machine learning algorithms to identify diagnostic and prognostic biomarkers associated with disulfidptosis in glioblastoma (GBM). First, we collected datas from TCGA and GTEx databases, and performed differential analysis, univariate Cox regression, and survival analysis. Additionally, we applied four machine learning algorithms to identify six candidate genes. We further investigated the potential biological functions and signaling pathways associated with these genes through GSEA and GSVA analysis. Subsequently, we constructed a ceRNA network and a drug-target network to explore their potential complex regulatory mechanisms. Finally, the expression levels of these genes were validated using clinical samples. Results show that these six candidate genes identified memorably, enriching in the JAK-STAT3 signaling pathway, were upregulated in glioblastoma (GBM) and were closely associated with patient prognosis. These findings may contribute to developing the molecular mechanisms underlying glioblastoma (GBM) and offer valuable implications for clinical diagnosis and treatment.

**Keywords: Bioinformatics, Glioblastoma, GBM, Disulfidptosis, JAK-STAT3, Diagnosis**

## 1. Introduction

Gliomas originate from glial cells in the brain and are among the most common primary malignant tumors in the brain(Qin et al., 2025). They are well-known for their high heterogeneity and high mortality rate(Zhao et al., 2023). According to the World Health Organization, gliomas are classified into grades I, II, III, and IV based on their malignancy, with higher grades indicating a greater degree of malignancy. GBM, classified as grade IV, represents the most malignant form of glioma. Additionally, the unique metabolic processes of GBM, such as glycolytic metabolism (Warburg effect) (Zhang et al., 2025)and choline metabolism(Ma et al., 2023), increase its danger. As a result, there is currently no effective treatment for GBM in clinical practice(Mandal, Banerjee, & Mandal, 2025). The first-line treatment involves surgical resection combined with adjuvant chemotherapy, but patient prognosis remains poor(Rodríguez-Camacho et al., 2022; Xu et al., 2025), with a median overall survival of only 4-18 months post-surgery(Tamai et al., 2022). Moreover, due to the development of drug resistance, the efficacy of temozolomide, an alkylating agent used as first-line treatment, has been increasingly limited(Lee et al., 2024).

Therefore, addressing these therapeutic challenges and identifying new effective treatments is crucial in clinical practice.

Disulfidptosis, a novel form of cell death distinct from ferroptosis, apoptosis, and other types, has been proposed in recent years. It is caused by excessive intracellular disulfide stress, leading to cell death(X. Liu et al., 2023). The mechanism of disulfide cell death involves the large-scale transport of cystine into cells through SLC7A11. Under conditions of glucose deprivation and lack of NADPH, a large accumulation of cystine and disulfides occurs within the cell, inducing a disulfide stress state, which ultimately triggers associated cell death(Goji, Takahara, Negishi, & Katoh, 2017; Joly, Delfarah, Phung, Parrish, & Graham, 2020; X. Liu et al., 2023). Although caspase-8 is involved in regulating this cell death process, it is different from the protective cell death forms like caspase-8-mediated apoptosis and necroptosis under normal physiological conditions(Tummers & Green, 2017). Based on this novel form of cell death, investigating disulfide death-related genes closely associated with GBM could help deepen our understanding of its pathogenesis, which holds significant implications for clinical diagnosis, treatment, and prognosis assessment.

This study utilizes bioinformatics techniques and various machine learning algorithms to screen for biomarkers associated with GBM. These findings will help us understand the role of disulfide-related cell death in the occurrence, development, and invasion of GBM and assist in further analyzing the molecular mechanisms of GBM progression, providing guidance for clinical diagnosis and treatment.

## Results

### Identification of Correlative Genes of DE-DSGs

Differential analysis was performed using TCGA GBM data and GTEx normal sample data, and a volcano plot of significantly different genes was constructed (**Figure1a**). Among the 16 disulfide death-related genes, 5 genes showed significant differential expression between TCGA GBM samples and GTEx normal samples, including 2 upregulated genes and 3 downregulated genes (**Figure1b,-c**). The goal is to further investigate genes potentially associated with disulfide-related mortality, correlation analysis was performed between these 5 genes and all genes in the TCGA GBM data, followed by Lasso and univariate Cox regression analyses, resulting in 24 independent prognostic genes (**Figure1d-f**). To further explore the biological functions and potential signaling pathways associated with these 24 genes, we performed Gene Ontology (GO) and Kyoto Encyclopedia of Genes and Genomes (KEGG) enrichment analyses. GO enrichment results (**Figure1g**) indicated that, in biological processes, these genes were mainly associated with T-cell regulation and protein tyrosine kinase regulation. In cellular components, they were primarily related to the endoplasmic reticulum and postsynaptic membranes. Molecular functions were primarily associated with cytokine receptors, growth factor binding, and ribonuclease activity. KEGG analysis (**Figure1h**) revealed that these genes were mainly involved in glycosaminoglycan biosynthesis, protein transport, and cytokine receptor interaction pathways. These analyses provided some insights for further investigation.

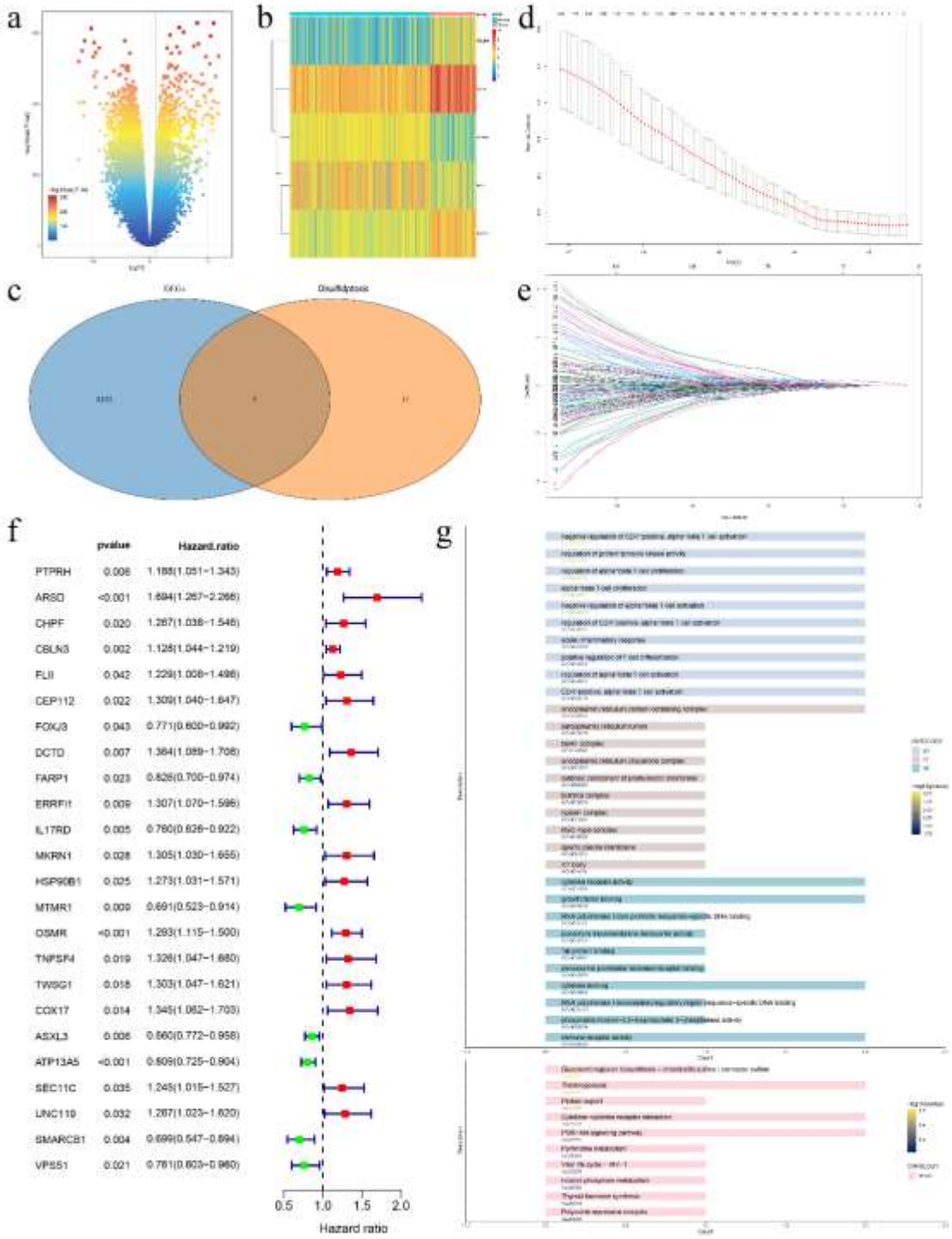


**Figure1 Identification of independent prognostic genes related to disulfidptosis in glioblastoma. a. Differential analysis of TCGA sample data and volcano plot; b-c. Intersection of differentially expressed genes with disulfidptosis-related genes and heatmap plotting; d-e. Lasso regression analysis to screen for correlated genes; f. Univariate correlation analysis further identifying independent prognostic genes related to disulfidptosis; g. GO and KEGG enrichment analysis to explore the potential biological processes and signaling pathways involved in these independent prognostic genes**

**Identification of Twelve Correlative Genes of DE-DSGs as Diagnostic Genes for GBM**

To further evaluate the diagnostic potential of these differentially expressed genes for GBM, we applied four machine learning algorithms to identify more representative genes. Using 10-fold

cross-validation with the Lasso regression algorithm, we identified 17 candidate genes (**Figure2a-c**). After analyzing the 24 genes using the XGBoost algorithm, 23 candidate genes were selected (**Figure2d**). Random Forest algorithm analysis of the 24 genes also selected genes that met the algorithm's criteria (**Figure2e-f**). SVM-RFE algorithm analysis revealed the smallest error rate at 16 iterations (Figure2g), leading to the selection of 16 candidate genes. Finally, 12 diagnostic genes identified by all four algorithms , for example, ARSD, ASXL3, CBLN3, DCTD, FOXJ3, IL17RD, OSMR, SEC11C, SMARCB1, TNFSF4, TWSG1, and UNC119, were selected for further analysis (**Figure2g**). Next, we constructed an ROC curve using these 12 diagnostic genes to assess the predictive performance of the SVM-RFE algorithm, which showed an AUC of 0.996 (**Figure3a**), indicating the reliability of the SVM-RFE model. Additionally, most of the AUC values were above 0.7 (**Figure3b**), suggesting that these genes have high diagnostic efficacy for GBM.

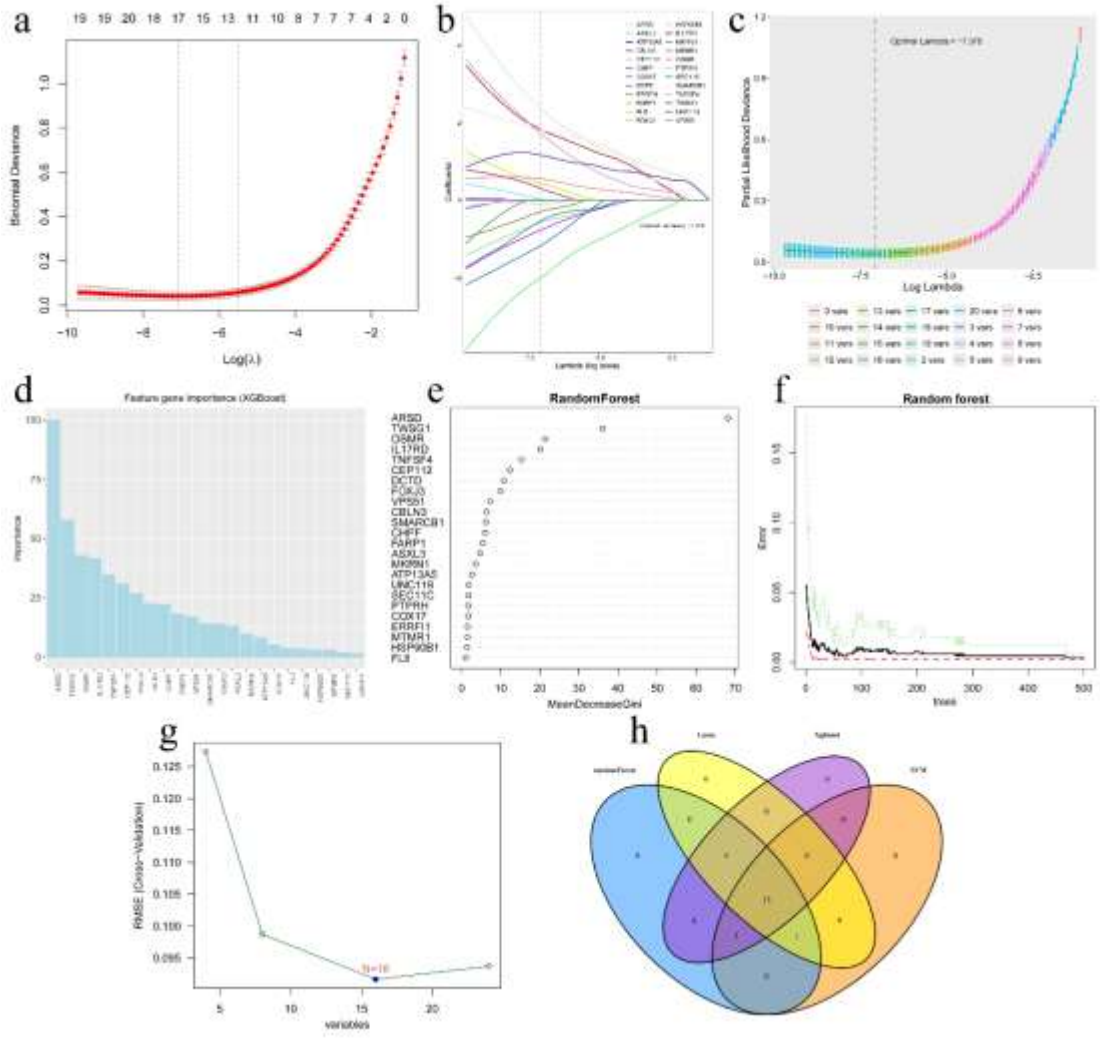


**Figure2 Further screening of biomarkers in glioblastoma using four machine learning algorithms. a-c. Lasso regression analysis for screening and identifying candidate genes; d. XGBoost algorithm for screening and identifying candidate genes; e-f. Random forest algorithm for screening and identifying candidate genes; g. SVM-RFE algorithm for screening and identifying candidate genes; h. Intersection of candidate genes identified by the four machine learning algorithms**

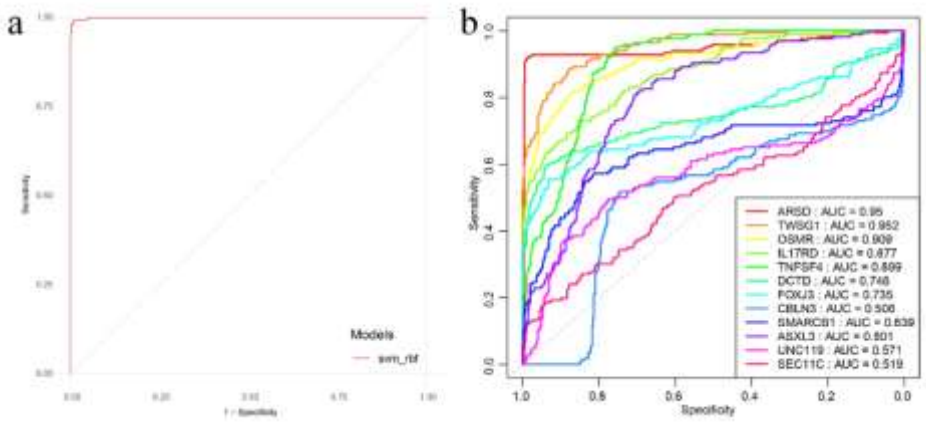


**Figure3 Evaluation of machine learning algorithm performance and construction of ROC curves for each candidate gene. a. Model construction to evaluate the performance of the SVM-RFE algorithm; b. Construction of ROC curves for the 12 candidate genes to evaluate their diagnostic performance**

### Survival Analysis of Twelve Signature Genes

To assess the impact of these 12 signature genes on GBM prognosis and further identify more meaningful diagnostic biomarkers, we conducted survival analysis using TCGA GBM data. As shown in Figure4, high expression of DCTD (p=0.014, HR=1.589, **Figure4a**), TWSG1 (p=0.009, HR=1.606, **Figure4b**), SEC11C (p=0.044, HR=1.458, **Figure4d**), and OSMR (p=0.010, HR=1.602, **Figure4e**) was associated with poorer prognosis in GBM patients, while low expression of IL17RD (p=0.010, HR=0.621, **Figure4c**) and SMARCB1 (p=0.009, HR=0.619, **Figure4f**) was linked to poorer prognosis. Additionally, ARSD (p=0.070, HR=1.402, **FigureS1a**), ASXL3 (p=0.114, HR=0.743, **FigureS1b**), CBLN3 (p=0.119, HR=1.336, **FigureS1c**), FOXJ3 (p=0.097, HR=0.734, **FigureS1d**), TNFSF4 (p=0.582, HR=1.11, **FigureS1e**), and UNC119 (p=0.151, HR=1.31, **FigureS1f**) showed no significant impact on the prognosis of GBM patients.

UNC119 (p=0.151, HR=1.31, **FigureS1f**) showed no significant impact on the prognosis of GBM patients.

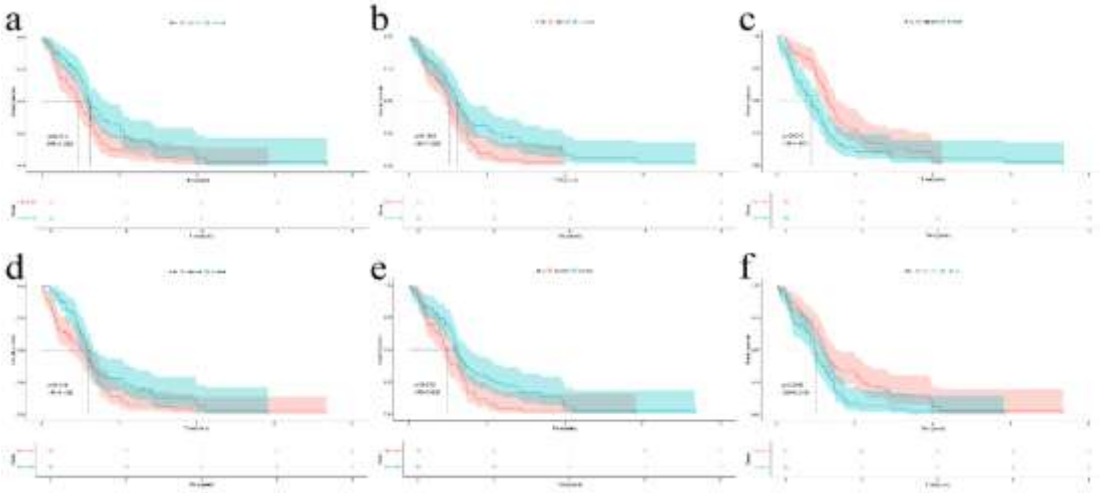


**Figure4 Kaplan-Meier survival analysis of the candidate genes and their prognostic significance for glioblastoma patients. a. DCTD; b. TWSG1; c. IL17RD; d. SEC11C; e. OSMR; f. SMARCB1**

**Association of Signature Diagnostic Genes with Oncogenic Pathways**

To further investigate the potential functional roles of these six prognostic genes, we performed GSEA pathway enrichment analysis. As shown in Figures5a-f, DCTD, TWSG1, OSMR, SMARCB1, and IL17RD were all enriched in the CYTOKINE_JAK_STAT3 Signaling Pathway and Translation Initiation signaling pathways. SMARCB1, IL17RD, and SEC11C were enriched in the Mitochondrial Complex UCP1 in Thermogenesis pathway. Additionally, they were associated with pathways such as ITGA_B_RHOG_RAC and ITGA_B_TALIN_VINCULIN.

We then conducted GSVA enrichment analysis to evaluate pathway activation patterns between high and low expression groups of each diagnostic gene. From Figure6, we observed that high expression levels of DCTD, OSMR, and TWSG1 were associated with activation of the IL6_JAK_STAT3 signaling pathway, interferon-related pathways, P53 signaling pathway, NFKB_TNFA signaling pathway, and apoptosis (**Figure6a-c**). Low expression levels of IL17RD and SMARCB1 were associated with the IL6_JAK_STAT3 signaling pathway, P53 signaling pathway, and apoptosis (**Figure6e-f**). Furthermore, high expression levels of SEC11C were primarily associated with oxidative phosphorylation, fatty acid metabolism, P53, and KRAS signaling pathways (**Figure6d**).

These results indicate that these six diagnostic genes are closely related to several tumor-related signaling pathways, including the JAK_STAT signaling pathway and P53 signaling pathway, both of which are crucial in tumorigenesis, progression, and diagnostic therapy. Notably, the JAK_STAT signaling pathway was highly correlated with DCTD, TWSG1, OSMR, SMARCB1, and IL17RD in both GSEA and GSVA analyses. These findings suggest that these diagnostic genes may regulate the biological processes of GBM through these signaling pathways.

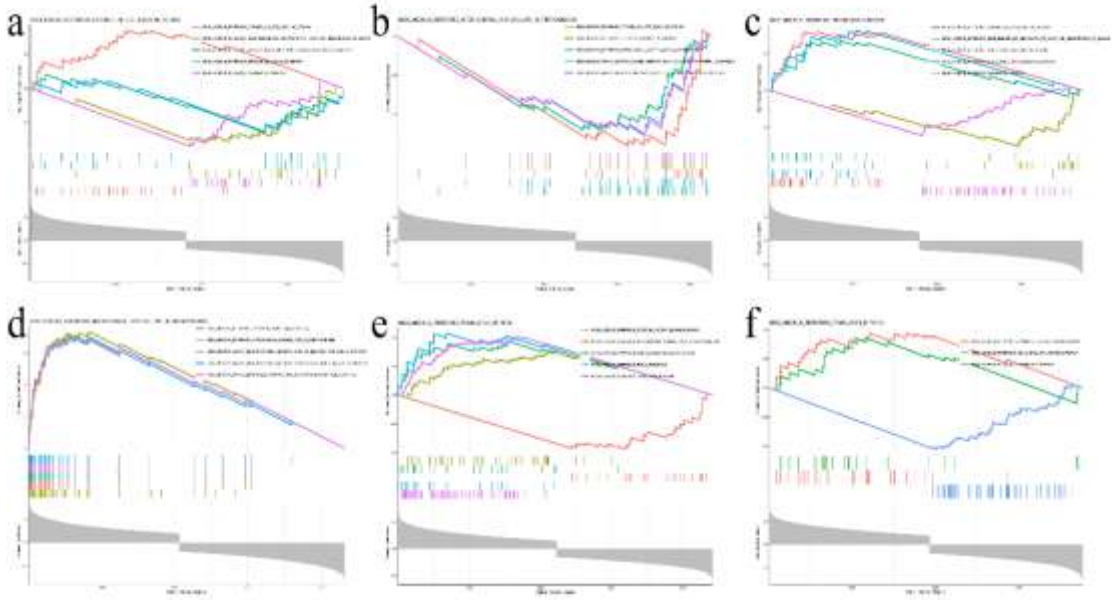


**Figure5 Single-gene GSEA signal pathway enrichment analysis of the six candidate genes with prognostic significance. a. DCTD; b. TWSG1; c. OSMR; d. SMARCB1; e. IL17RD; f. SEC11C**

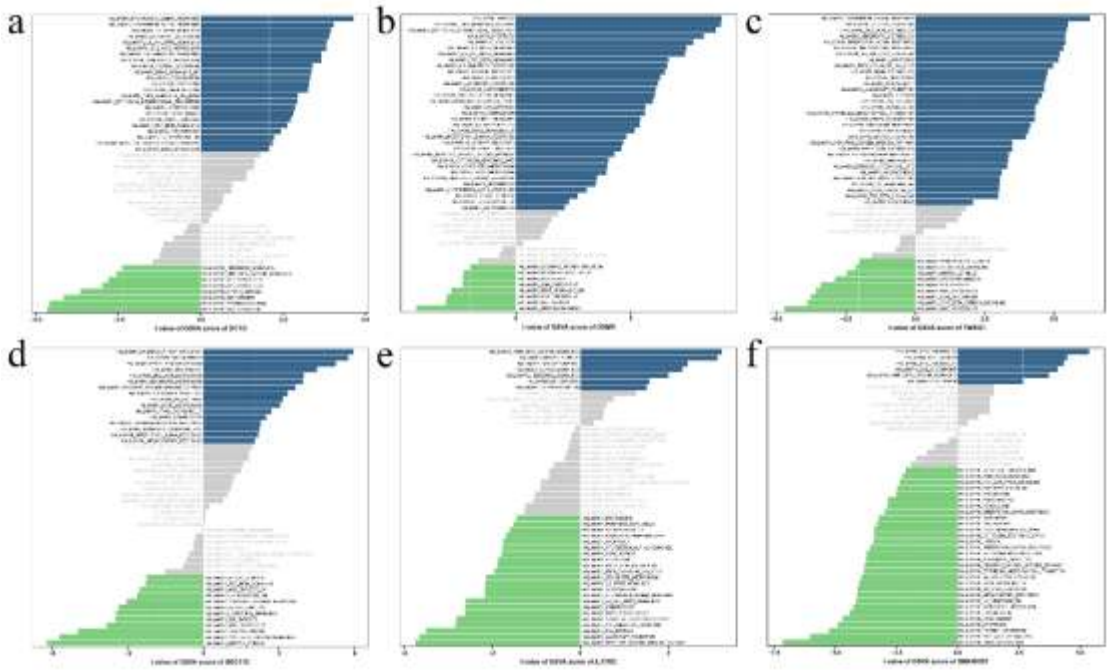


**Figure6 Single-gene GSVA analysis of the six candidate genes with prognostic significance to explore their potential relationship with classical tumor-related signaling pathways. a. DCTD; b. OSMR; c. TWSG1; d. SEC11C; e. IL17RD; f. SMARCB1**

### Differential Analysis of Signaling Pathways and Their Correlation with Marker Genes

To further investigate whether these potential signaling pathways exhibit differential expression between GBM and normal samples and assess the correlation of these pathways with marker genes, we performed differential analysis on the GSVA scores using the limma package and evaluated their association with the marker genes. A volcano plot of differential signaling pathways between GBM and normal samples was generated, with the top five signaling pathways of high and low expression annotated (**Figure7a**). The E2F_TARGETS, G2M_CHECKPOINT, INTERFERON_GAMMA_RESPONSE, INTERFERON_ALPHA_RESPONSE, and IL6_JAK_STAT3 pathways were highly expressed in GBM, while KRAS, HEDGEHOG signaling pathways, and oxidative phosphorylation showed a trend of low expression. In Figure7b, we found that DCTD, OSMR, and TWSG1 were positively correlated with multiple cancer-related signaling pathways, such as the IL6_JAK_STAT3 signaling pathway, P53 signaling pathway, PI3K_AKT_MTOR signaling pathway, and apoptosis signaling pathway. Conversely, IL17RD and SMARCB1 showed negative correlations with these pathways. Furthermore, SEC11C was primarily positively correlated with the P53 signaling pathway, bile acid metabolism, and oxidative phosphorylation pathways. These results further confirm previous findings, suggesting that these diagnostic genes may regulate the progression of GBM through these signaling pathways, potentially serving as therapeutic targets for GBM.

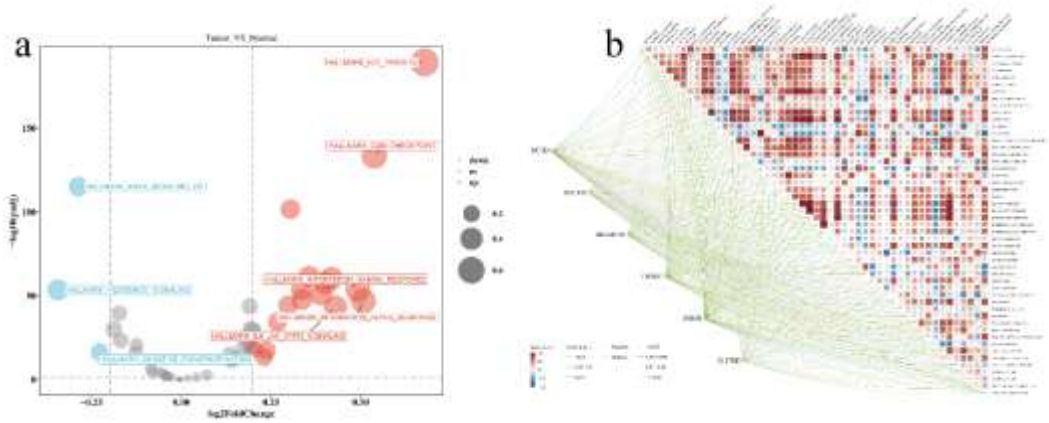


**Figure7 Differential analysis of signaling pathways in glioblastoma and normal samples and the correlation between the six candidate genes and these signaling pathways. a. Analysis of differential expression of these signaling pathways in glioblastoma and normal samples with a volcano plot; b. Heatmap of the correlation between the six candidate genes and each signaling pathway**

### Prediction of Targeted Therapeutics and Construction of ceRNA Networks

To further explore potential targeted drugs acting on these six genes, we used the DGIdb database to predict the target drugs for these genes, followed by visualization of the drug-gene interactions using Cytoscape software (**Figure8a**). A total of 68 drugs were identified, with the drug prediction results shown in **Table S3**.

**Table S3**.

| Medicine | Gene |
|---|---|
| Chlortetracycline | OSMR |
| 0316684-0000 | OSMR |
| Ciclopirox | OSMR |
| 5109870 | OSMR |
| Doxifluridine | OSMR |
| Tamoxifen | OSMR |
| Ciglitazone | OSMR |
| Tetradioxin | OSMR |
| Gefitinib | OSMR |
| Cadmium | OSMR |
| Estradiol | OSMR |
| Paclitaxel | OSMR |
| Tretinoin | OSMR |
| Benzo(a)pyrene | OSMR |
| Sarin | OSMR |
| Acetaminophen | OSMR |
| Aflatoxin B1 | OSMR |
| Cyclosporin A | OSMR |
| Irinotecan hydrochloride | OSMR |
| Deptropine | TWSG1 |
| Cinoxacin | TWSG1 |
| Vorinostat | TWSG1 |
| Scriptaid | TWSG1 |

| | |
|---|---|
| Helveticoside | TWSG1 |
| Trichostatin A | TWSG1 |
| Arsenite | TWSG1 |
| Copper sulfate | TWSG1 |
| Acetaminophen | TWSG1 |
| Cobaltous chloride | TWSG1 |
| Aflatoxin B1 | TWSG1 |
| Rifabutin | SMARCB1 |
| Vorinostat | SMARCB1 |
| Trichostatin A | SMARCB1 |
| Scriptaid | SMARCB1 |
| Sucrose | SMARCB1 |
| Artemisinin | SMARCB1 |
| Dichloromethane | SMARCB1 |
| 2,2',3',4,4',5-hexachlorobiphenyl | SMARCB1 |
| Epigallocatechin gallate | SMARCB1 |
| Potassium chromate(VI) | SMARCB1 |
| 3,4,5,3',4'-pentachlorobiphenyl | SMARCB1 |
| Valproic acid | SMARCB1 |
| Sulpiride | DCTD |
| Chlortetracycline | DCTD |
| Chlorzoxazone | DCTD |
| Cimetidine | DCTD |
| Cefadroxil | DCTD |
| Chlorhexidine | DCTD |
| PHA-00665752 | DCTD |
| Captopril | DCTD |
| Vorinostat | DCTD |
| Azacyclonol | DCTD |
| Dirithromycin | DCTD |
| Medrysone | DCTD |
| Ampyrone | DCTD |
| Clopamide | DCTD |
| Deptropine | DCTD |
| Trichostatin A | DCTD |
| Lobeline | DCTD |
| Ajmaline | DCTD |
| Clindamycin | DCTD |
| Glibenclamide | DCTD |
| Meclofenoxate | DCTD |
| Danazol | DCTD |
| Scriptaid | DCTD |
| PNU-0293363 | DCTD |
| 0175029-0000 | DCTD |
| Gemcitavine hydrochloride | DCTD |
| Paclitaxel | DCTD |
| Cobaltous chloride | DCTD |
| Cyclosporin A | DCTD |
| Valproic Acid | DCTD |
| Quercetin | SEC11C |
| Copper | SEC11C |
| Hydralazine | SEC11C |

| | |
|---|---|
| Thapsigargin | SEC11C |
| Cycloheximide | SEC11C |
| Tetradioxin | SEC11C |
| Copper sulfate | SEC11C |
| Retinoic acid | SEC11C |
| Acetaminophen | SEC11C |
| Cyclosporin A | SEC11C |
| Valproic Acid | SEC11C |
| Bortezomib | IL17RD |
| Hydrogen peroxide | IL17RD |
| Estradiol | IL17RD |
| Mono-(2-ethylhexyl)phthalate | IL17RD |
| Trichostatin A | IL17RD |
| Valproic Acid | IL17RD |
| Progesterone | IL17RD |

Specifically, OSMR was predicted to interact with 19 drugs, TWSG1 with 11 drugs, SMARCB1 with 12 drugs, DCTD with 30 drugs, SEC11C with 11 drugs, and IL17RD with 7 drugs.

Next, we predicted the miRNAs and lncRNAs associated with these marker genes using the miRDB, TargetScan, and starBase databases, constructing a lncRNA-miRNA-mRNA regulatory network (**Figure8b**). This network included 258 nodes, comprising the 6 marker genes, 44 miRNAs, and 208 lncRNAs. A total of 225 lncRNAs were found to competitively bind 6 miRNAs (including hsa-miR-3619-5p, hsa-miR-214-3p) to regulate IL17RD. Among them, 52 lncRNAs competed with hsa-miR-3619-5p, and 51 lncRNAs competed with hsa-miR-214-3p. Additionally, 82 lncRNAs competed with two miRNAs (including hsa-miR-3163 and hsa-miR-340-5p) to regulate TWSG1, with 56 lncRNAs targeting hsa-miR-3163 and 26 lncRNAs targeting hsa-miR-340-5p. Moreover, 26 lncRNAs regulated DCTD by competitively binding hsa-miR-516b-5b, and 40 lncRNAs targeted hsa-miR-3118 to regulate OSMR. However, no lncRNAs were found to regulate SMARCB1 and SEC11C. Detailed interactions are listed in Table S4 and Table S5.

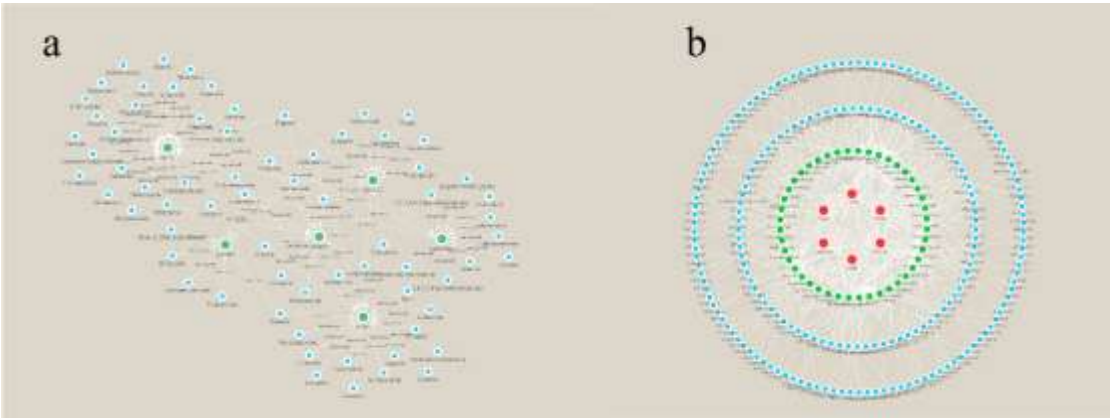


**Figure8 Use of databases to predict target drugs for each gene and the construction of a network diagram of lncRNA-miRNA-mRNA interactions to explore their more complex regulatory mechanisms. a. Network diagram showing the relationship between each candidate gene and its**

**targeted drugs; b. Construct a network diagram of the interaction between lncRNA, miRNA, and mRNA**

**Table s4**

| Source | Target |
|---|---|
| hsa-miR-3163 | TWSG1 |
| hsa-miR-340-5p | TWSG1 |
| hsa-miR-5694 | TWSG1 |
| hsa-miR-6128 | TWSG1 |
| hsa-miR-4282 | TWSG1 |
| hsa-miR-4528 | TWSG1 |
| hsa-miR-548t-3p | TWSG1 |
| hsa-miR-548aa | TWSG1 |
| hsa-miR-548ap-3p | TWSG1 |
| hsa-miR-1299 | TWSG1 |
| hsa-miR-664a-3p | TWSG1 |
| hsa-miR-4477a | TWSG1 |
| MIR29B2CHG | hsa-miR-340-5p |
| THUMPD3-AS1 | hsa-miR-340-5p |
| AC093010.2 | hsa-miR-340-5p |
| SLC26A4-AS1 | hsa-miR-340-5p |
| AC090739.1 | hsa-miR-340-5p |
| ERICD | hsa-miR-340-5p |
| AL158206.1 | hsa-miR-340-5p |
| EBLN3P | hsa-miR-340-5p |
| SNHG1 | hsa-miR-340-5p |
| NEAT1 | hsa-miR-340-5p |
| AC026356.1 | hsa-miR-340-5p |
| TRHDE-AS1 | hsa-miR-340-5p |
| HELLPAR | hsa-miR-340-5p |
| AC108704.2 | hsa-miR-340-5p |
| SNHG14 | hsa-miR-340-5p |
| OIP5-AS1 | hsa-miR-340-5p |
| DNAAF4-CCPG1 | hsa-miR-340-5p |
| AC021483.2 | hsa-miR-340-5p |
| AC020978.7 | hsa-miR-340-5p |
| CCDC144NL-AS1 | hsa-miR-340-5p |
| LINC00662 | hsa-miR-340-5p |
| AC008555.6 | hsa-miR-340-5p |
| AC005261.1 | hsa-miR-340-5p |
| LINC01694 | hsa-miR-340-5p |
| XIST | hsa-miR-340-5p |
| LINC00630 | hsa-miR-340-5p |
| Z99943.1 | hsa-miR-3163 |
| DNM3OS | hsa-miR-3163 |
| TNR-IT1 | hsa-miR-3163 |
| AC012358.1 | hsa-miR-3163 |
| CHROMR | hsa-miR-3163 |
| KANSL1L-AS1 | hsa-miR-3163 |
| AC016717.2 | hsa-miR-3163 |
| FGD5-AS1 | hsa-miR-3163 |

| | |
|---|---|
| AC096921.2 | hsa-miR-3163 |
| AC022336.2 | hsa-miR-3163 |
| AC093866.1 | hsa-miR-3163 |
| AC010261.2 | hsa-miR-3163 |
| AC021078.1 | hsa-miR-3163 |
| AL031779.1 | hsa-miR-3163 |
| LINC00472 | hsa-miR-3163 |
| MANEA-DT | hsa-miR-3163 |
| AC007036.3 | hsa-miR-3163 |
| MAGI2-AS3 | hsa-miR-3163 |
| AC000123.3 | hsa-miR-3163 |
| AC004908.3 | hsa-miR-3163 |
| OTUD6B-AS1 | hsa-miR-3163 |
| ARRDC1-AS1 | hsa-miR-3163 |
| AL132656.4 | hsa-miR-3163 |
| OLMALINC | hsa-miR-3163 |
| KCNQ1OT1 | hsa-miR-3163 |
| SNHG1 | hsa-miR-3163 |
| NEAT1 | hsa-miR-3163 |
| MALAT1 | hsa-miR-3163 |
| MIR100HG | hsa-miR-3163 |
| AC008124.1 | hsa-miR-3163 |
| AL445223.1 | hsa-miR-3163 |
| AL356019.2 | hsa-miR-3163 |
| PSMA3-AS1 | hsa-miR-3163 |
| SNHG14 | hsa-miR-3163 |
| OIP5-AS1 | hsa-miR-3163 |
| AC051619.6 | hsa-miR-3163 |
| DNAAF4-CCPG1 | hsa-miR-3163 |
| ST20-AS1 | hsa-miR-3163 |
| CHASERR | hsa-miR-3163 |
| AC092718.3 | hsa-miR-3163 |
| AC133540.1 | hsa-miR-3163 |
| FAM106A | hsa-miR-3163 |
| LINC02693 | hsa-miR-3163 |
| AC125257.1 | hsa-miR-3163 |
| AC006141.1 | hsa-miR-3163 |
| AC018628.1 | hsa-miR-3163 |
| SNHG16 | hsa-miR-3163 |
| AC243964.4 | hsa-miR-3163 |
| AC005261.1 | hsa-miR-3163 |
| NORAD | hsa-miR-3163 |
| DSCAM-AS1 | hsa-miR-3163 |
| LINC01311 | hsa-miR-3163 |
| AP000553.2 | hsa-miR-3163 |
| MIR222HG | hsa-miR-3163 |
| XIST | hsa-miR-3163 |
| Z83843.1 | hsa-miR-3163 |
| hsa-miR-516b-5p | DCTD |
| hsa-miR-1304-5p | DCTD |
| hsa-miR-1252-3p | DCTD |
| hsa-miR-892b | DCTD |

| | |
|---|---|
| AL645608.7 | hsa-miR-516b-5p |
| AL590666.2 | hsa-miR-516b-5p |
| AL691482.3 | hsa-miR-516b-5p |
| PCBP1-AS1 | hsa-miR-516b-5p |
| LINC01123 | hsa-miR-516b-5p |
| LINC01106 | hsa-miR-516b-5p |
| PAX8-AS1 | hsa-miR-516b-5p |
| LINC01184 | hsa-miR-516b-5p |
| LINC02487 | hsa-miR-516b-5p |
| AC079781.5 | hsa-miR-516b-5p |
| SND1-IT1 | hsa-miR-516b-5p |
| AC016065.1 | hsa-miR-516b-5p |
| RPARP-AS1 | hsa-miR-516b-5p |
| H19 | hsa-miR-516b-5p |
| KCNQ1OT1 | hsa-miR-516b-5p |
| NEAT1 | hsa-miR-516b-5p |
| HELLPAR | hsa-miR-516b-5p |
| AC131212.3 | hsa-miR-516b-5p |
| LINC00641 | hsa-miR-516b-5p |
| AC092718.6 | hsa-miR-516b-5p |
| AC092127.1 | hsa-miR-516b-5p |
| AC016876.2 | hsa-miR-516b-5p |
| LINC00324 | hsa-miR-516b-5p |
| TBC1D3P1-DHX40P1 | hsa-miR-516b-5p |
| DLGAP1-AS2 | hsa-miR-516b-5p |
| MIR23AHG | hsa-miR-516b-5p |
| AL133325.3 | hsa-miR-516b-5p |
| GUSBP11 | hsa-miR-516b-5p |
| MIAT | hsa-miR-516b-5p |
| hsa-miR-6809-3p | IL17RD |
| hsa-miR-22-3p | IL17RD |
| hsa-miR-4441 | IL17RD |
| hsa-miR-6878-3p | IL17RD |
| hsa-miR-6736-3p | IL17RD |
| hsa-miR-6754-5p | IL17RD |
| hsa-miR-761 | IL17RD |
| hsa-miR-3619-5p | IL17RD |
| hsa-miR-193a-3p | IL17RD |
| hsa-miR-214-3p | IL17RD |
| hsa-miR-4270 | IL17RD |
| hsa-miR-193b-3p | IL17RD |
| hsa-let-7c-3p | IL17RD |
| hsa-miR-4291 | IL17RD |
| hsa-miR-7160-5p | IL17RD |
| hsa-miR-3613-3p | IL17RD |
| MIR34AHG | hsa-miR-22-3p |
| LINC00339 | hsa-miR-22-3p |
| AL360012.1 | hsa-miR-22-3p |
| AL162431.1 | hsa-miR-22-3p |
| AC119427.2 | hsa-miR-22-3p |
| AC005538.2 | hsa-miR-22-3p |
| FGD5-AS1 | hsa-miR-22-3p |

| | |
|---|---|
| SH3BP5-AS1 | hsa-miR-22-3p |
| AC079228.1 | hsa-miR-22-3p |
| AC021078.1 | hsa-miR-22-3p |
| SLC25A25-AS1 | hsa-miR-22-3p |
| LINC00963 | hsa-miR-22-3p |
| AL390294.1 | hsa-miR-22-3p |
| H19 | hsa-miR-22-3p |
| AC091564.7 | hsa-miR-22-3p |
| NEAT1 | hsa-miR-22-3p |
| MALAT1 | hsa-miR-22-3p |
| COLCA1 | hsa-miR-22-3p |
| SNHG14 | hsa-miR-22-3p |
| PWAR5 | hsa-miR-22-3p |
| AC022613.1 | hsa-miR-22-3p |
| OIP5-AS1 | hsa-miR-22-3p |
| Z92544.1 | hsa-miR-22-3p |
| AC009133.1 | hsa-miR-22-3p |
| AC135048.1 | hsa-miR-22-3p |
| SNHG29 | hsa-miR-22-3p |
| SNHG16 | hsa-miR-22-3p |
| AC087741.1 | hsa-miR-22-3p |
| NORAD | hsa-miR-22-3p |
| GUSBP11 | hsa-miR-22-3p |
| AL008721.2 | hsa-miR-22-3p |
| MIRLET7BHG | hsa-miR-22-3p |
| LINC00630 | hsa-miR-22-3p |
| Z68871.1 | hsa-miR-22-3p |
| AL162431.1 | hsa-miR-193a-3p |
| CYTOR | hsa-miR-193a-3p |
| MIR4435-2HG | hsa-miR-193a-3p |
| AC017002.3 | hsa-miR-193a-3p |
| LINC01184 | hsa-miR-193a-3p |
| AL353795.3 | hsa-miR-193a-3p |
| SNHG7 | hsa-miR-193a-3p |
| KCNQ1OT1 | hsa-miR-193a-3p |
| MIR194-2HG | hsa-miR-193a-3p |
| NEAT1 | hsa-miR-193a-3p |
| AP001273.1 | hsa-miR-193a-3p |
| LINC01089 | hsa-miR-193a-3p |
| AC135050.6 | hsa-miR-193a-3p |
| AC010327.6 | hsa-miR-193a-3p |
| ZFAS1 | hsa-miR-193a-3p |
| MIRLET7BHG | hsa-miR-193a-3p |
| XIST | hsa-miR-193a-3p |
| AL162431.1 | hsa-miR-193b-3p |
| CYTOR | hsa-miR-193b-3p |
| MIR4435-2HG | hsa-miR-193b-3p |
| AC017002.3 | hsa-miR-193b-3p |
| LINC01184 | hsa-miR-193b-3p |
| AL353795.3 | hsa-miR-193b-3p |
| SNHG7 | hsa-miR-193b-3p |
| KCNQ1OT1 | hsa-miR-193b-3p |

| | |
|---|---|
| MIR194-2HG | hsa-miR-193b-3p |
| NEAT1 | hsa-miR-193b-3p |
| AP001273.1 | hsa-miR-193b-3p |
| LINC01089 | hsa-miR-193b-3p |
| AC135050.6 | hsa-miR-193b-3p |
| AC092295.2 | hsa-miR-193b-3p |
| AC010327.6 | hsa-miR-193b-3p |
| ZFAS1 | hsa-miR-193b-3p |
| MIRLET7BHG | hsa-miR-193b-3p |
| XIST | hsa-miR-193b-3p |
| AL645608.2 | hsa-miR-214-3p |
| AL031282.2 | hsa-miR-214-3p |
| MIR34AHG | hsa-miR-214-3p |
| LINC00339 | hsa-miR-214-3p |
| SLFNL1-AS1 | hsa-miR-214-3p |
| LINC01140 | hsa-miR-214-3p |
| MIR29B2CHG | hsa-miR-214-3p |
| AL160408.3 | hsa-miR-214-3p |
| AC012513.3 | hsa-miR-214-3p |
| LINC02832 | hsa-miR-214-3p |
| FGD5-AS1 | hsa-miR-214-3p |
| TMCC1-AS1 | hsa-miR-214-3p |
| PP7080 | hsa-miR-214-3p |
| SLC9A3-AS1 | hsa-miR-214-3p |
| TMEM161B-AS1 | hsa-miR-214-3p |
| EPB41L4A-AS1 | hsa-miR-214-3p |
| CASC15 | hsa-miR-214-3p |
| CT66 | hsa-miR-214-3p |
| STAG3L5P-PVRIG2P-PILRB | hsa-miR-214-3p |
| AC069281.2 | hsa-miR-214-3p |
| AP003472.2 | hsa-miR-214-3p |
| AC084125.2 | hsa-miR-214-3p |
| AL157392.3 | hsa-miR-214-3p |
| AP006621.5 | hsa-miR-214-3p |
| KCNQ1OT1 | hsa-miR-214-3p |
| NEAT1 | hsa-miR-214-3p |
| AP003119.3 | hsa-miR-214-3p |
| AC026362.1 | hsa-miR-214-3p |
| MIR17HG | hsa-miR-214-3p |
| LINC00641 | hsa-miR-214-3p |
| Z98883.1 | hsa-miR-214-3p |
| AC106820.4 | hsa-miR-214-3p |
| AC020663.4 | hsa-miR-214-3p |
| AC109460.3 | hsa-miR-214-3p |
| SLX1A-SULT1A3 | hsa-miR-214-3p |
| AC113189.4 | hsa-miR-214-3p |
| AC055811.4 | hsa-miR-214-3p |
| SNHG16 | hsa-miR-214-3p |
| AC087741.1 | hsa-miR-214-3p |
| LINC00482 | hsa-miR-214-3p |
| LINC01535 | hsa-miR-214-3p |
| AC093227.1 | hsa-miR-214-3p |

| | |
|---|---|
| PCAT19 | hsa-miR-214-3p |
| A1BG-AS1 | hsa-miR-214-3p |
| AL121906.2 | hsa-miR-214-3p |
| SNHG17 | hsa-miR-214-3p |
| TSPEAR-AS2 | hsa-miR-214-3p |
| AC002470.2 | hsa-miR-214-3p |
| MIRLET7BHG | hsa-miR-214-3p |
| C22orf34 | hsa-miR-214-3p |
| XIST | hsa-miR-214-3p |
| AL645608.2 | hsa-miR-761 |
| AL031282.2 | hsa-miR-761 |
| MIR34AHG | hsa-miR-761 |
| LINC00339 | hsa-miR-761 |
| SLFNL1-AS1 | hsa-miR-761 |
| LINC01140 | hsa-miR-761 |
| MIR29B2CHG | hsa-miR-761 |
| AL160408.3 | hsa-miR-761 |
| AC012513.3 | hsa-miR-761 |
| LINC02832 | hsa-miR-761 |
| FGD5-AS1 | hsa-miR-761 |
| TMCC1-AS1 | hsa-miR-761 |
| PP7080 | hsa-miR-761 |
| SLC9A3-AS1 | hsa-miR-761 |
| TMEM161B-AS1 | hsa-miR-761 |
| EPB41L4A-AS1 | hsa-miR-761 |
| CASC15 | hsa-miR-761 |
| CT66 | hsa-miR-761 |
| STAG3L5P-PVRIG2P-PILRB | hsa-miR-761 |
| AC069281.2 | hsa-miR-761 |
| AP003472.2 | hsa-miR-761 |
| AC084125.2 | hsa-miR-761 |
| AL157392.3 | hsa-miR-761 |
| SGMS1-AS1 | hsa-miR-761 |
| AP006621.5 | hsa-miR-761 |
| KCNQ1OT1 | hsa-miR-761 |
| NEAT1 | hsa-miR-761 |
| AP003119.3 | hsa-miR-761 |
| AC026362.1 | hsa-miR-761 |
| MIR17HG | hsa-miR-761 |
| LINC00641 | hsa-miR-761 |
| Z98883.1 | hsa-miR-761 |
| AC106820.4 | hsa-miR-761 |
| AC020663.4 | hsa-miR-761 |
| AC109460.3 | hsa-miR-761 |
| SLX1A-SULT1A3 | hsa-miR-761 |
| AC113189.4 | hsa-miR-761 |
| AC055811.4 | hsa-miR-761 |
| SNHG16 | hsa-miR-761 |
| AC087741.1 | hsa-miR-761 |
| LINC00482 | hsa-miR-761 |
| LINC01535 | hsa-miR-761 |
| AC093227.1 | hsa-miR-761 |

| | |
|---|---|
| PCAT19 | hsa-miR-761 |
| AC073548.1 | hsa-miR-761 |
| A1BG-AS1 | hsa-miR-761 |
| AL121906.2 | hsa-miR-761 |
| SNHG17 | hsa-miR-761 |
| TSPEAR-AS2 | hsa-miR-761 |
| AC002470.2 | hsa-miR-761 |
| MIRLET7BHG | hsa-miR-761 |
| C22orf34 | hsa-miR-761 |
| XIST | hsa-miR-761 |
| AL645608.2 | hsa-miR-3619-5p |
| AL031282.2 | hsa-miR-3619-5p |
| MIR34AHG | hsa-miR-3619-5p |
| LINC00339 | hsa-miR-3619-5p |
| SLFNL1-AS1 | hsa-miR-3619-5p |
| LINC01140 | hsa-miR-3619-5p |
| MIR29B2CHG | hsa-miR-3619-5p |
| AL160408.3 | hsa-miR-3619-5p |
| AC012513.3 | hsa-miR-3619-5p |
| LINC02832 | hsa-miR-3619-5p |
| FGD5-AS1 | hsa-miR-3619-5p |
| TMCC1-AS1 | hsa-miR-3619-5p |
| PP7080 | hsa-miR-3619-5p |
| SLC9A3-AS1 | hsa-miR-3619-5p |
| TMEM161B-AS1 | hsa-miR-3619-5p |
| EPB41L4A-AS1 | hsa-miR-3619-5p |
| CASC15 | hsa-miR-3619-5p |
| CT66 | hsa-miR-3619-5p |
| STAG3L5P-PVRIG2P-PILRB | hsa-miR-3619-5p |
| AC069281.2 | hsa-miR-3619-5p |
| AP003472.2 | hsa-miR-3619-5p |
| AC084125.2 | hsa-miR-3619-5p |
| AL157392.3 | hsa-miR-3619-5p |
| SGMS1-AS1 | hsa-miR-3619-5p |
| KCNQ1OT1 | hsa-miR-3619-5p |
| NEAT1 | hsa-miR-3619-5p |
| AP003119.3 | hsa-miR-3619-5p |
| AC026362.1 | hsa-miR-3619-5p |
| MIR17HG | hsa-miR-3619-5p |
| LINC00641 | hsa-miR-3619-5p |
| Z98883.1 | hsa-miR-3619-5p |
| AC106820.4 | hsa-miR-3619-5p |
| AC020663.4 | hsa-miR-3619-5p |
| AC109460.3 | hsa-miR-3619-5p |
| SLX1A-SULT1A3 | hsa-miR-3619-5p |
| AC113189.4 | hsa-miR-3619-5p |
| AC055811.4 | hsa-miR-3619-5p |
| SNHG16 | hsa-miR-3619-5p |
| AC087741.1 | hsa-miR-3619-5p |
| LINC00482 | hsa-miR-3619-5p |
| LINC01535 | hsa-miR-3619-5p |
| AC093227.1 | hsa-miR-3619-5p |

| | |
|---|---|
| PCAT19 | hsa-miR-3619-5p |
| AC073548.1 | hsa-miR-3619-5p |
| A1BG-AS1 | hsa-miR-3619-5p |
| AL121906.2 | hsa-miR-3619-5p |
| SNHG17 | hsa-miR-3619-5p |
| TSPEAR-AS2 | hsa-miR-3619-5p |
| AC002470.2 | hsa-miR-3619-5p |
| MIRLET7BHG | hsa-miR-3619-5p |
| C22orf34 | hsa-miR-3619-5p |
| XIST | hsa-miR-3619-5p |
| hsa-miR-4504 | OSMR |
| hsa-miR-518c-5p | OSMR |
| hsa-miR-3118 | OSMR |
| hsa-miR-100-3p | OSMR |
| hsa-miR-4501 | OSMR |
| PINK1-AS | hsa-miR-3118 |
| AL445231.1 | hsa-miR-3118 |
| ADAMTSL4-AS1 | hsa-miR-3118 |
| DNM3OS | hsa-miR-3118 |
| HK2-DT | hsa-miR-3118 |
| LINC01123 | hsa-miR-3118 |
| LINC01106 | hsa-miR-3118 |
| AC009948.1 | hsa-miR-3118 |
| LINC01963 | hsa-miR-3118 |
| AC104447.1 | hsa-miR-3118 |
| LINC02035 | hsa-miR-3118 |
| LINC01618 | hsa-miR-3118 |
| PP7080 | hsa-miR-3118 |
| SND1-IT1 | hsa-miR-3118 |
| AC007938.3 | hsa-miR-3118 |
| CDKN2B-AS1 | hsa-miR-3118 |
| AL353795.3 | hsa-miR-3118 |
| MIR600HG | hsa-miR-3118 |
| OLMALINC | hsa-miR-3118 |
| KCNQ1OT1 | hsa-miR-3118 |
| NEAT1 | hsa-miR-3118 |
| AC005831.1 | hsa-miR-3118 |
| AC144548.1 | hsa-miR-3118 |
| AC073592.5 | hsa-miR-3118 |
| Z92544.1 | hsa-miR-3118 |
| MIR22HG | hsa-miR-3118 |
| AC015799.1 | hsa-miR-3118 |
| AC127521.1 | hsa-miR-3118 |
| LINC02693 | hsa-miR-3118 |
| AC005562.1 | hsa-miR-3118 |
| AC004687.1 | hsa-miR-3118 |
| AC005332.6 | hsa-miR-3118 |
| AC145207.5 | hsa-miR-3118 |
| TYMSOS | hsa-miR-3118 |
| WDR7-OT1 | hsa-miR-3118 |
| MIR122HG | hsa-miR-3118 |
| AC007191.1 | hsa-miR-3118 |

| | |
|---|---|
| AL117335.1 | hsa-miR-3118 |
| LINC01278 | hsa-miR-3118 |
| FTX | hsa-miR-3118 |
| hsa-miR-4520-2-3p | SEC11C |
| hsa-miR-1185-1-3p | SEC11C |
| hsa-miR-1185-2-3p | SEC11C |
| hsa-let-7f-2-3p | SEC11C |
| hsa-miR-372-5p | SEC11C |
| hsa-miR-6832-3p | SEC11C |
| hsa-miR-4283 | SMARCB1 |

Table S5

| Source | Type |
|---|---|
| DCTD | mRNA-DCTD |
| hsa-miR-516b-5p | miRNA-DCTD |
| hsa-miR-1304-5p | miRNA-DCTD |
| hsa-miR-1252-3p | miRNA-DCTD |
| hsa-miR-892b | miRNA-DCTD |
| AL645608.7 | lncRNA-DCTD |
| AL590666.2 | lncRNA-DCTD |
| AL691482.3 | lncRNA-DCTD |
| PCBP1-AS1 | lncRNA-DCTD |
| LINC01123 | lncRNA-DCTD |
| LINC01106 | lncRNA-DCTD |
| PAX8-AS1 | lncRNA-DCTD |
| LINC01184 | lncRNA-DCTD |
| LINC02487 | lncRNA-DCTD |
| AC079781.5 | lncRNA-DCTD |
| SND1-IT1 | lncRNA-DCTD |
| AC016065.1 | lncRNA-DCTD |
| RPARP-AS1 | lncRNA-DCTD |
| H19 | lncRNA-DCTD |
| KCNQ1OT1 | lncRNA-DCTD |
| NEAT1 | lncRNA-DCTD |
| HELLPAR | lncRNA-DCTD |
| AC131212.3 | lncRNA-DCTD |
| LINC00641 | lncRNA-DCTD |
| AC092718.6 | lncRNA-DCTD |
| AC092127.1 | lncRNA-DCTD |
| AC016876.2 | lncRNA-DCTD |
| LINC00324 | lncRNA-DCTD |
| TBC1D3P1-DHX40P1 | lncRNA-DCTD |
| DLGAP1-AS2 | lncRNA-DCTD |
| MIR23AHG | lncRNA-DCTD |
| AL133325.3 | lncRNA-DCTD |
| GUSBP11 | lncRNA-DCTD |
| MIAT | lncRNA-DCTD |
| IL17RD | mRNA-IL17RD |
| hsa-miR-6809-3p | miRNA-IL17RD |
| hsa-miR-22-3p | miRNA-IL17RD |
| hsa-miR-4441 | miRNA-IL17RD |

| | |
|---|---|
| hsa-miR-6878-3p | miRNA-IL17RD |
| hsa-miR-6736-3p | miRNA-IL17RD |
| hsa-miR-6754-5p | miRNA-IL17RD |
| hsa-miR-761 | miRNA-IL17RD |
| hsa-miR-3619-5p | miRNA-IL17RD |
| hsa-miR-193a-3p | miRNA-IL17RD |
| hsa-miR-214-3p | miRNA-IL17RD |
| hsa-miR-4270 | miRNA-IL17RD |
| hsa-miR-193b-3p | miRNA-IL17RD |
| hsa-let-7c-3p | miRNA-IL17RD |
| hsa-miR-4291 | miRNA-IL17RD |
| hsa-miR-7160-5p | miRNA-IL17RD |
| hsa-miR-3613-3p | miRNA-IL17RD |
| MIR34AHG | lncRNA-IL17RD |
| LINC00339 | lncRNA-IL17RD |
| AL360012.1 | lncRNA-IL17RD |
| AL162431.1 | lncRNA-IL17RD |
| AC119427.2 | lncRNA-IL17RD |
| AC005538.2 | lncRNA-IL17RD |
| FGD5-AS1 | lncRNA-IL17RD |
| SH3BP5-AS1 | lncRNA-IL17RD |
| AC079228.1 | lncRNA-IL17RD |
| AC021078.1 | lncRNA-IL17RD |
| SLC25A25-AS1 | lncRNA-IL17RD |
| LINC00963 | lncRNA-IL17RD |
| AL390294.1 | lncRNA-IL17RD |
| H19 | lncRNA-IL17RD |
| AC091564.7 | lncRNA-IL17RD |
| NEAT1 | lncRNA-IL17RD |
| MALAT1 | lncRNA-IL17RD |
| COLCA1 | lncRNA-IL17RD |
| SNHG14 | lncRNA-IL17RD |
| PWAR5 | lncRNA-IL17RD |
| AC022613.1 | lncRNA-IL17RD |
| OIP5-AS1 | lncRNA-IL17RD |
| Z92544.1 | lncRNA-IL17RD |
| AC009133.1 | lncRNA-IL17RD |
| AC135048.1 | lncRNA-IL17RD |
| SNHG29 | lncRNA-IL17RD |
| SNHG16 | lncRNA-IL17RD |
| AC087741.1 | lncRNA-IL17RD |
| NORAD | lncRNA-IL17RD |
| GUSBP11 | lncRNA-IL17RD |
| AL008721.2 | lncRNA-IL17RD |
| MIRLET7BHG | lncRNA-IL17RD |
| LINC00630 | lncRNA-IL17RD |
| Z68871.1 | lncRNA-IL17RD |
| AL162431.1 | lncRNA-IL17RD |
| CYTOR | lncRNA-IL17RD |
| MIR4435-2HG | lncRNA-IL17RD |
| AC017002.3 | lncRNA-IL17RD |
| LINC01184 | lncRNA-IL17RD |

| | |
|---|---|
| AL353795.3 | lncRNA-IL17RD |
| SNHG7 | lncRNA-IL17RD |
| KCNQ1OT1 | lncRNA-IL17RD |
| MIR194-2HG | lncRNA-IL17RD |
| NEAT1 | lncRNA-IL17RD |
| AP001273.1 | lncRNA-IL17RD |
| LINC01089 | lncRNA-IL17RD |
| AC135050.6 | lncRNA-IL17RD |
| AC010327.6 | lncRNA-IL17RD |
| ZFAS1 | lncRNA-IL17RD |
| MIRLET7BHG | lncRNA-IL17RD |
| XIST | lncRNA-IL17RD |
| AL162431.1 | lncRNA-IL17RD |
| CYTOR | lncRNA-IL17RD |
| MIR4435-2HG | lncRNA-IL17RD |
| AC017002.3 | lncRNA-IL17RD |
| LINC01184 | lncRNA-IL17RD |
| AL353795.3 | lncRNA-IL17RD |
| SNHG7 | lncRNA-IL17RD |
| KCNQ1OT1 | lncRNA-IL17RD |
| MIR194-2HG | lncRNA-IL17RD |
| NEAT1 | lncRNA-IL17RD |
| AP001273.1 | lncRNA-IL17RD |
| LINC01089 | lncRNA-IL17RD |
| AC135050.6 | lncRNA-IL17RD |
| AC092295.2 | lncRNA-IL17RD |
| AC010327.6 | lncRNA-IL17RD |
| ZFAS1 | lncRNA-IL17RD |
| MIRLET7BHG | lncRNA-IL17RD |
| XIST | lncRNA-IL17RD |
| AL645608.2 | lncRNA-IL17RD |
| AL031282.2 | lncRNA-IL17RD |
| MIR34AHG | lncRNA-IL17RD |
| LINC00339 | lncRNA-IL17RD |
| SLFNL1-AS1 | lncRNA-IL17RD |
| LINC01140 | lncRNA-IL17RD |
| MIR29B2CHG | lncRNA-IL17RD |
| AL160408.3 | lncRNA-IL17RD |
| AC012513.3 | lncRNA-IL17RD |
| LINC02832 | lncRNA-IL17RD |
| FGD5-AS1 | lncRNA-IL17RD |
| TMCC1-AS1 | lncRNA-IL17RD |
| PP7080 | lncRNA-IL17RD |
| SLC9A3-AS1 | lncRNA-IL17RD |
| TMEM161B-AS1 | lncRNA-IL17RD |
| EPB41L4A-AS1 | lncRNA-IL17RD |
| CASC15 | lncRNA-IL17RD |
| CT66 | lncRNA-IL17RD |
| STAG3L5P-PVRIG2P-PILRB | lncRNA-IL17RD |
| AC069281.2 | lncRNA-IL17RD |
| AP003472.2 | lncRNA-IL17RD |
| AC084125.2 | lncRNA-IL17RD |

| | |
|---|---|
| AL157392.3 | lncRNA-IL17RD |
| AP006621.5 | lncRNA-IL17RD |
| KCNQ1OT1 | lncRNA-IL17RD |
| NEAT1 | lncRNA-IL17RD |
| AP003119.3 | lncRNA-IL17RD |
| AC026362.1 | lncRNA-IL17RD |
| MIR17HG | lncRNA-IL17RD |
| LINC00641 | lncRNA-IL17RD |
| Z98883.1 | lncRNA-IL17RD |
| AC106820.4 | lncRNA-IL17RD |
| AC020663.4 | lncRNA-IL17RD |
| AC109460.3 | lncRNA-IL17RD |
| SLX1A-SULT1A3 | lncRNA-IL17RD |
| AC113189.4 | lncRNA-IL17RD |
| AC055811.4 | lncRNA-IL17RD |
| SNHG16 | lncRNA-IL17RD |
| AC087741.1 | lncRNA-IL17RD |
| LINC00482 | lncRNA-IL17RD |
| LINC01535 | lncRNA-IL17RD |
| AC093227.1 | lncRNA-IL17RD |
| PCAT19 | lncRNA-IL17RD |
| A1BG-AS1 | lncRNA-IL17RD |
| AL121906.2 | lncRNA-IL17RD |
| SNHG17 | lncRNA-IL17RD |
| TSPEAR-AS2 | lncRNA-IL17RD |
| AC002470.2 | lncRNA-IL17RD |
| MIRLET7BHG | lncRNA-IL17RD |
| C22orf34 | lncRNA-IL17RD |
| XIST | lncRNA-IL17RD |
| AL645608.2 | lncRNA-IL17RD |
| AL031282.2 | lncRNA-IL17RD |
| MIR34AHG | lncRNA-IL17RD |
| LINC00339 | lncRNA-IL17RD |
| SLFNL1-AS1 | lncRNA-IL17RD |
| LINC01140 | lncRNA-IL17RD |
| MIR29B2CHG | lncRNA-IL17RD |
| AL160408.3 | lncRNA-IL17RD |
| AC012513.3 | lncRNA-IL17RD |
| LINC02832 | lncRNA-IL17RD |
| FGD5-AS1 | lncRNA-IL17RD |
| TMCC1-AS1 | lncRNA-IL17RD |
| PP7080 | lncRNA-IL17RD |
| SLC9A3-AS1 | lncRNA-IL17RD |
| TMEM161B-AS1 | lncRNA-IL17RD |
| EPB41L4A-AS1 | lncRNA-IL17RD |
| CASC15 | lncRNA-IL17RD |
| CT66 | lncRNA-IL17RD |
| STAG3L5P-PVRIG2P-PILRB | lncRNA-IL17RD |
| AC069281.2 | lncRNA-IL17RD |
| AP003472.2 | lncRNA-IL17RD |
| AC084125.2 | lncRNA-IL17RD |
| AL157392.3 | lncRNA-IL17RD |

| | |
|---|---|
| SGMS1-AS1 | lncRNA-IL17RD |
| AP006621.5 | lncRNA-IL17RD |
| KCNQ1OT1 | lncRNA-IL17RD |
| NEAT1 | lncRNA-IL17RD |
| AP003119.3 | lncRNA-IL17RD |
| AC026362.1 | lncRNA-IL17RD |
| MIR17HG | lncRNA-IL17RD |
| LINC00641 | lncRNA-IL17RD |
| Z98883.1 | lncRNA-IL17RD |
| AC106820.4 | lncRNA-IL17RD |
| AC020663.4 | lncRNA-IL17RD |
| AC109460.3 | lncRNA-IL17RD |
| SLX1A-SULT1A3 | lncRNA-IL17RD |
| AC113189.4 | lncRNA-IL17RD |
| AC055811.4 | lncRNA-IL17RD |
| SNHG16 | lncRNA-IL17RD |
| AC087741.1 | lncRNA-IL17RD |
| LINC00482 | lncRNA-IL17RD |
| LINC01535 | lncRNA-IL17RD |
| AC093227.1 | lncRNA-IL17RD |
| PCAT19 | lncRNA-IL17RD |
| AC073548.1 | lncRNA-IL17RD |
| A1BG-AS1 | lncRNA-IL17RD |
| AL121906.2 | lncRNA-IL17RD |
| SNHG17 | lncRNA-IL17RD |
| TSPEAR-AS2 | lncRNA-IL17RD |
| AC002470.2 | lncRNA-IL17RD |
| MIRLET7BHG | lncRNA-IL17RD |
| C22orf34 | lncRNA-IL17RD |
| XIST | lncRNA-IL17RD |
| AL645608.2 | lncRNA-IL17RD |
| AL031282.2 | lncRNA-IL17RD |
| MIR34AHG | lncRNA-IL17RD |
| LINC00339 | lncRNA-IL17RD |
| SLFNL1-AS1 | lncRNA-IL17RD |
| LINC01140 | lncRNA-IL17RD |
| MIR29B2CHG | lncRNA-IL17RD |
| AL160408.3 | lncRNA-IL17RD |
| AC012513.3 | lncRNA-IL17RD |
| LINC02832 | lncRNA-IL17RD |
| FGD5-AS1 | lncRNA-IL17RD |
| TMCC1-AS1 | lncRNA-IL17RD |
| PP7080 | lncRNA-IL17RD |
| SLC9A3-AS1 | lncRNA-IL17RD |
| TMEM161B-AS1 | lncRNA-IL17RD |
| EPB41L4A-AS1 | lncRNA-IL17RD |
| CASC15 | lncRNA-IL17RD |
| CT66 | lncRNA-IL17RD |
| STAG3L5P-PVRIG2P-PILRB | lncRNA-IL17RD |
| AC069281.2 | lncRNA-IL17RD |
| AP003472.2 | lncRNA-IL17RD |
| AC084125.2 | lncRNA-IL17RD |

| | |
|---|---|
| AL157392.3 | lncRNA-IL17RD |
| SGMS1-AS1 | lncRNA-IL17RD |
| KCNQ1OT1 | lncRNA-IL17RD |
| NEAT1 | lncRNA-IL17RD |
| AP003119.3 | lncRNA-IL17RD |
| AC026362.1 | lncRNA-IL17RD |
| MIR17HG | lncRNA-IL17RD |
| LINC00641 | lncRNA-IL17RD |
| Z98883.1 | lncRNA-IL17RD |
| AC106820.4 | lncRNA-IL17RD |
| AC020663.4 | lncRNA-IL17RD |
| AC109460.3 | lncRNA-IL17RD |
| SLX1A-SULT1A3 | lncRNA-IL17RD |
| AC113189.4 | lncRNA-IL17RD |
| AC055811.4 | lncRNA-IL17RD |
| SNHG16 | lncRNA-IL17RD |
| AC087741.1 | lncRNA-IL17RD |
| LINC00482 | lncRNA-IL17RD |
| LINC01535 | lncRNA-IL17RD |
| AC093227.1 | lncRNA-IL17RD |
| PCAT19 | lncRNA-IL17RD |
| AC073548.1 | lncRNA-IL17RD |
| A1BG-AS1 | lncRNA-IL17RD |
| AL121906.2 | lncRNA-IL17RD |
| SNHG17 | lncRNA-IL17RD |
| TSPEAR-AS2 | lncRNA-IL17RD |
| AC002470.2 | lncRNA-IL17RD |
| MIRLET7BHG | lncRNA-IL17RD |
| C22orf34 | lncRNA-IL17RD |
| XIST | lncRNA-IL17RD |
| OSMR | mRNA-OSMR |
| hsa-miR-4504 | miRNA-OSMR |
| hsa-miR-518c-5p | miRNA-OSMR |
| hsa-miR-3118 | miRNA-OSMR |
| hsa-miR-100-3p | miRNA-OSMR |
| hsa-miR-4501 | miRNA-OSMR |
| PINK1-AS | lncRNA-OSMR |
| AL445231.1 | lncRNA-OSMR |
| ADAMTSL4-AS1 | lncRNA-OSMR |
| DNM3OS | lncRNA-OSMR |
| HK2-DT | lncRNA-OSMR |
| LINC01123 | lncRNA-OSMR |
| LINC01106 | lncRNA-OSMR |
| AC009948.1 | lncRNA-OSMR |
| LINC01963 | lncRNA-OSMR |
| AC104447.1 | lncRNA-OSMR |
| LINC02035 | lncRNA-OSMR |
| LINC01618 | lncRNA-OSMR |
| PP7080 | lncRNA-OSMR |
| SND1-IT1 | lncRNA-OSMR |
| AC007938.3 | lncRNA-OSMR |
| CDKN2B-AS1 | lncRNA-OSMR |

| | |
|---|---|
| AL353795.3 | lncRNA-OSMR |
| MIR600HG | lncRNA-OSMR |
| OLMALINC | lncRNA-OSMR |
| KCNQ1OT1 | lncRNA-OSMR |
| NEAT1 | lncRNA-OSMR |
| AC005831.1 | lncRNA-OSMR |
| AC144548.1 | lncRNA-OSMR |
| AC073592.5 | lncRNA-OSMR |
| Z92544.1 | lncRNA-OSMR |
| MIR22HG | lncRNA-OSMR |
| AC015799.1 | lncRNA-OSMR |
| AC127521.1 | lncRNA-OSMR |
| LINC02693 | lncRNA-OSMR |
| AC005562.1 | lncRNA-OSMR |
| AC004687.1 | lncRNA-OSMR |
| AC005332.6 | lncRNA-OSMR |
| AC145207.5 | lncRNA-OSMR |
| TYMSOS | lncRNA-OSMR |
| WDR7-OT1 | lncRNA-OSMR |
| MIR122HG | lncRNA-OSMR |
| AC007191.1 | lncRNA-OSMR |
| AL117335.1 | lncRNA-OSMR |
| LINC01278 | lncRNA-OSMR |
| FTX | lncRNA-OSMR |
| SEC11C | mRNA-SEC11C |
| hsa-miR-4520-2-3p | miRNA-SEC11C |
| hsa-miR-1185-1-3p | miRNA-SEC11C |
| hsa-miR-1185-2-3p | miRNA-SEC11C |
| hsa-let-7f-2-3p | miRNA-SEC11C |
| hsa-miR-372-5p | miRNA-SEC11C |
| hsa-miR-6832-3p | miRNA-SEC11C |
| SMARCB1 | mRNA-SMARCB1 |
| hsa-miR-4283 | miRNA-SMARCB1 |
| TWSG1 | mRNA-TWSG1 |
| hsa-miR-3163 | miRNA-TWSG1 |
| hsa-miR-340-5p | miRNA-TWSG1 |
| hsa-miR-5694 | miRNA-TWSG1 |
| hsa-miR-6128 | miRNA-TWSG1 |
| hsa-miR-4282 | miRNA-TWSG1 |
| hsa-miR-4528 | miRNA-TWSG1 |
| hsa-miR-548t-3p | miRNA-TWSG1 |
| hsa-miR-548aa | miRNA-TWSG1 |
| hsa-miR-548ap-3p | miRNA-TWSG1 |
| hsa-miR-1299 | miRNA-TWSG1 |
| hsa-miR-664a-3p | miRNA-TWSG1 |
| hsa-miR-4477a | miRNA-TWSG1 |
| MIR29B2CHG | lncRNA-TWSG1 |
| THUMPD3-AS1 | lncRNA-TWSG1 |
| AC093010.2 | lncRNA-TWSG1 |
| SLC26A4-AS1 | lncRNA-TWSG1 |
| AC090739.1 | lncRNA-TWSG1 |
| ERICD | lncRNA-TWSG1 |

| | |
|---|---|
| AL158206.1 | lncRNA-TWSG1 |
| EBLN3P | lncRNA-TWSG1 |
| SNHG1 | lncRNA-TWSG1 |
| NEAT1 | lncRNA-TWSG1 |
| AC026356.1 | lncRNA-TWSG1 |
| TRHDE-AS1 | lncRNA-TWSG1 |
| HELLPAR | lncRNA-TWSG1 |
| AC108704.2 | lncRNA-TWSG1 |
| SNHG14 | lncRNA-TWSG1 |
| OIP5-AS1 | lncRNA-TWSG1 |
| DNAAF4-CCPG1 | lncRNA-TWSG1 |
| AC021483.2 | lncRNA-TWSG1 |
| AC020978.7 | lncRNA-TWSG1 |
| CCDC144NL-AS1 | lncRNA-TWSG1 |
| LINC00662 | lncRNA-TWSG1 |
| AC008555.6 | lncRNA-TWSG1 |
| AC005261.1 | lncRNA-TWSG1 |
| LINC01694 | lncRNA-TWSG1 |
| XIST | lncRNA-TWSG1 |
| LINC00630 | lncRNA-TWSG1 |
| Z99943.1 | lncRNA-TWSG1 |
| DNM3OS | lncRNA-TWSG1 |
| TNR-IT1 | lncRNA-TWSG1 |
| AC012358.1 | lncRNA-TWSG1 |
| CHROMR | lncRNA-TWSG1 |
| KANSL1L-AS1 | lncRNA-TWSG1 |
| AC016717.2 | lncRNA-TWSG1 |
| FGD5-AS1 | lncRNA-TWSG1 |
| AC096921.2 | lncRNA-TWSG1 |
| AC022336.2 | lncRNA-TWSG1 |
| AC093866.1 | lncRNA-TWSG1 |
| AC010261.2 | lncRNA-TWSG1 |
| AC021078.1 | lncRNA-TWSG1 |
| AL031779.1 | lncRNA-TWSG1 |
| LINC00472 | lncRNA-TWSG1 |
| MANEA-DT | lncRNA-TWSG1 |
| AC007036.3 | lncRNA-TWSG1 |
| MAGI2-AS3 | lncRNA-TWSG1 |
| AC000123.3 | lncRNA-TWSG1 |
| AC004908.3 | lncRNA-TWSG1 |
| OTUD6B-AS1 | lncRNA-TWSG1 |
| ARRDC1-AS1 | lncRNA-TWSG1 |
| AL132656.4 | lncRNA-TWSG1 |
| OLMALINC | lncRNA-TWSG1 |
| KCNQ1OT1 | lncRNA-TWSG1 |
| SNHG1 | lncRNA-TWSG1 |
| NEAT1 | lncRNA-TWSG1 |
| MALAT1 | lncRNA-TWSG1 |
| MIR100HG | lncRNA-TWSG1 |
| AC008124.1 | lncRNA-TWSG1 |
| AL445223.1 | lncRNA-TWSG1 |
| AL356019.2 | lncRNA-TWSG1 |

| | |
|---|---|
| PSMA3-AS1 | lncRNA-TWSG1 |
| SNHG14 | lncRNA-TWSG1 |
| OIP5-AS1 | lncRNA-TWSG1 |
| AC051619.6 | lncRNA-TWSG1 |
| DNAAF4-CCPG1 | lncRNA-TWSG1 |
| ST20-AS1 | lncRNA-TWSG1 |
| CHASERR | lncRNA-TWSG1 |
| AC092718.3 | lncRNA-TWSG1 |
| AC133540.1 | lncRNA-TWSG1 |
| FAM106A | lncRNA-TWSG1 |
| LINC02693 | lncRNA-TWSG1 |
| AC125257.1 | lncRNA-TWSG1 |
| AC006141.1 | lncRNA-TWSG1 |
| AC018628.1 | lncRNA-TWSG1 |
| SNHG16 | lncRNA-TWSG1 |
| AC243964.4 | lncRNA-TWSG1 |
| AC005261.1 | lncRNA-TWSG1 |
| NORAD | lncRNA-TWSG1 |
| DSCAM-AS1 | lncRNA-TWSG1 |
| LINC01311 | lncRNA-TWSG1 |
| AP000553.2 | lncRNA-TWSG1 |
| MIR222HG | lncRNA-TWSG1 |
| XIST | lncRNA-TWSG1 |
| Z83843.1 | lncRNA-TWSG1 |

**Validation Using the Independent Validation Cohort**

Finally, we used the GSE4290 dataset to validate the expression of these 6 marker genes in GBM and normal samples. Additionally, we used the GSE43378 and GSE83300 datasets to validate the survival analysis of these 6 marker genes in GBM patients. In the TCGA and GTEx merged data, we found that DCTD, SMARCB1, TWSG1, OSMR, and IL17RD were all highly expressed in GBM, while SEC11C showed no significant correlation (**Figure9a**). In the GSE4290 dataset, all 6 marker genes exhibited a trend of high expression in GBM (**Figure9b**), which was consistent with the test set results. The survival analysis results in the GSE43378 and GSE83300 validation datasets showed that, except for DCTD ($p=0.101$, HR=1.424, **Figure9c**) and SEC11C ($p=0.232$, HR=0.773, **Figure9d**), which had no significant correlation, IL17RD ($p=0.030$, HR=0.63, **Figure9e**), TWSG1 ($p=0.003$, HR=1.895, **Figure9f**), OSMR ($p=0.017$, HR=1.666, **Figure9g**), and SMARCB1 ($p<0.001$, HR=0.46, **Figure9h**) had significant effects on the prognosis of GBM patients.

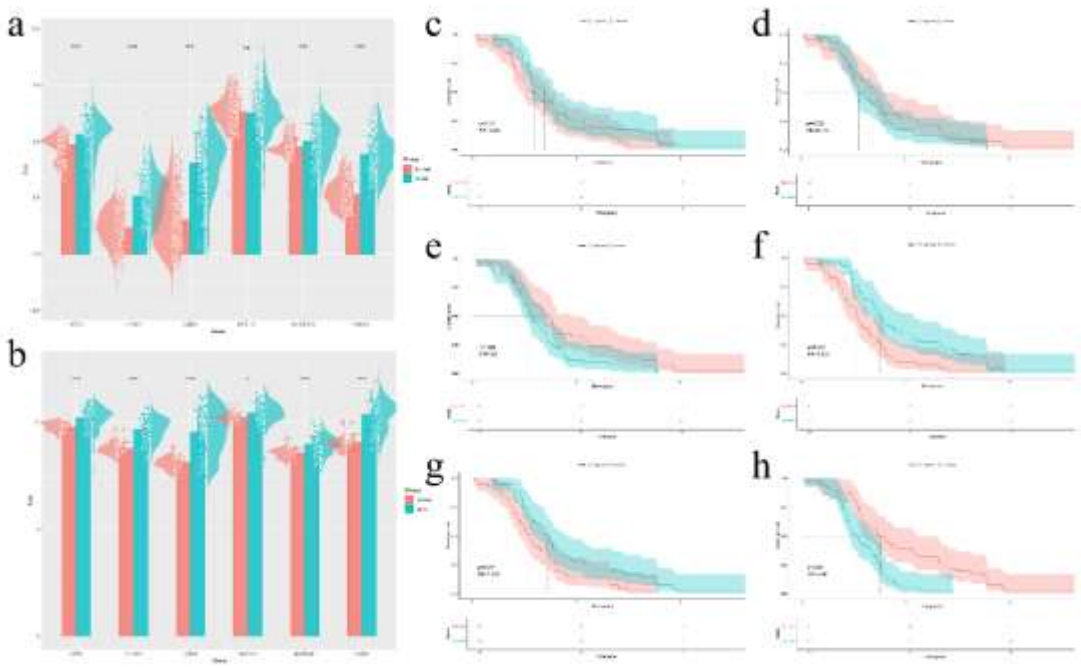


**Figure9 Validation of the above analysis results using the GEO dataset. a. Analysis of the expression levels of each candidate gene using TCGA glioblastoma data and GTEx normal sample data; b. Validation of the expression levels of each candidate gene using the GEO validation dataset; c-h. Further analysis of the prognostic impact of each gene on glioblastoma patients in the GEO dataset and construction of Kaplan-Meier survival curves**

### Validation of Marker Genes Expression Levels in Clinical GBM Samples

To further validate the practical applicability of these marker genes, we collected clinical GBM samples and adjacent tumor tissues for fluorescent quantitative PCR validation. Using GraphPad and performing T-test analysis, the results showed that DCTD ($p=0.0123$), SEC11C ($p<0.0001$), OSMR ($p=0.0465$), SMARCB1 ($p=0.0392$), TWSG1 ($p=0.0019$), and IL17RD ($p=0.0035$) were all relatively highly expressed in GBM tissues (**Figure10a-f**), which was consistent with the previous bioinformatics analysis results, indicating that these marker genes hold significant potential implications for the diagnosis and clinical treatment of GBM.

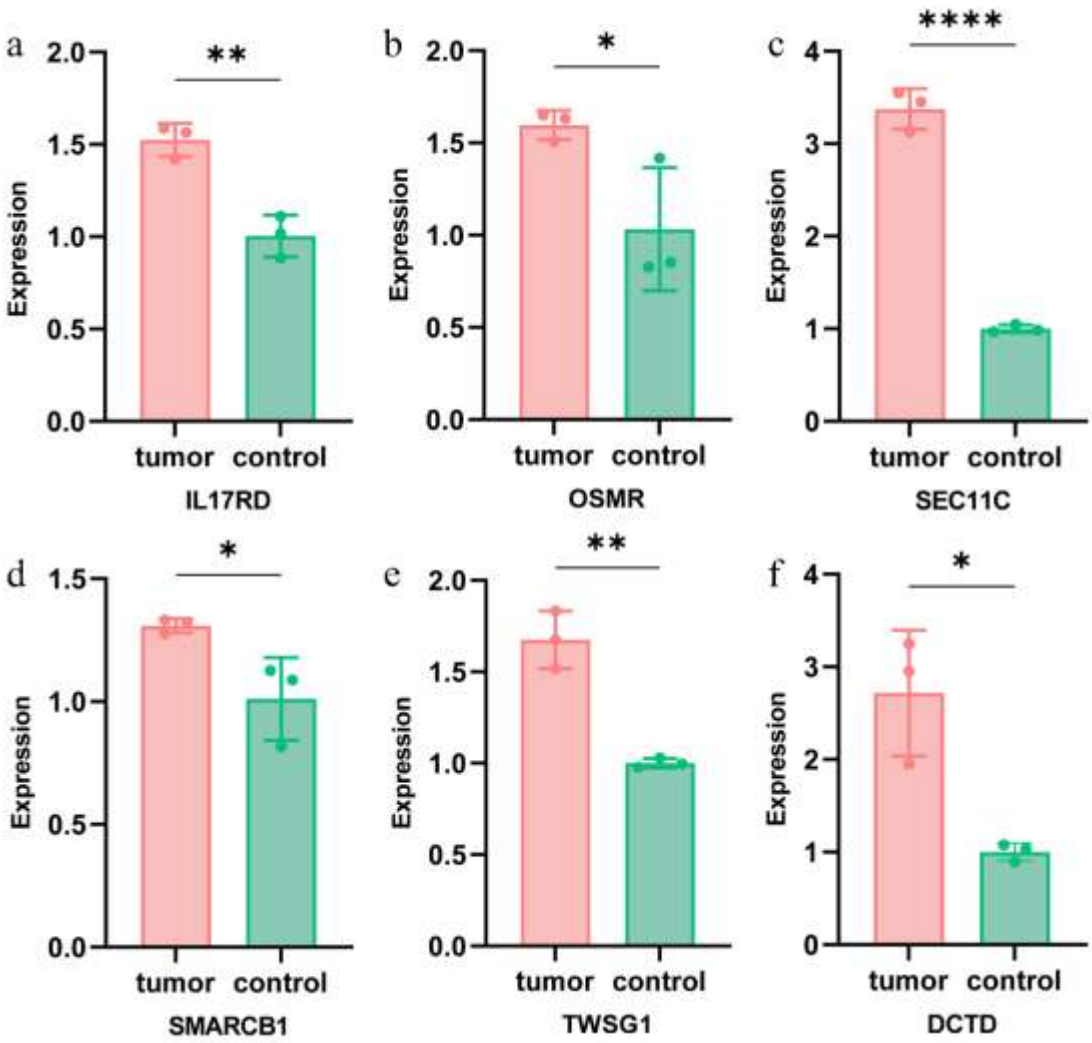


**Figure10 Quantitative PCR validation of the expression levels of each candidate gene using clinical glioblastoma samples. a-f. IL17RD, OSMR, SEC11C, SMARCB1, TWSG1, and DCTD respectively**

## Materials and Methods

### Data Acquisition and Preprocessing

All original analysis data for this study were obtained from the TCGA, UCSC Xena, and GEO databases. We downloaded data from 176 GBM samples (including 172 tumor samples and 4 normal samples) along with clinical phenotype data from TCGA (https://portal.gdc.cancer.gov/) and extracted RNA-seq expression data in Transcripts Per Million (TPM) format. We excluded samples from the clinical phenotype data that lacked survival status or survival time and retained sample names, survival status, and survival time, resulting in 160 clinical samples. We then downloaded the normal brain tissue expression data (in TPM format) and phenotype data from the GTEx database (https://xenabrowser.net/datapages/). The GBM data from TCGA and the normal brain tissue data from GTEx (500 normal samples) were merged, batch effects were removed, and the data were normalized and log2-transformed to create the test set. Furthermore, we downloaded the GSE43378, GSE4290, and GSE83300 datasets from the GEO database (https://www.ncbi.nlm.nih.gov/geo/) for validation. Additionally, 16 disulfide cell death-related genes(H. Liu & Tang, 2023) were obtained from the literature for subsequent analysis.

**Differential Analysis and Selection of Independent Prognostic Genes**

We performed differential analysis using the merged TCGA GBM data and GTEx normal data in R 4.4.0 with the limma package to identify differentially expressed genes (DEGs). In the analysis, the thresholds for selection were set at an adjusted p-value < 0.05 and |log2(FC)| > 1. We then intersected the obtained DEGs with the 16 disulfide death genes to identify differentially expressed disulfide death genes. These genes were further analyzed through Pearson correlation analysis with all genes, selecting genes with correlation coefficients R > 0.5 and p-values < 0.05. The Lasso analysis of these correlated genes was performed using the glmnet package in R, and the optimal cross-validation result was obtained at $\lambda$ = -2.681073. Subsequently, a univariate analysis model was constructed using the patients' survival status and survival time to further screen for independent prognostic genes. Genes with a p-value < 0.05 from the univariate analysis were included in the subsequent analysis.

**Multiple Machine Learning Algorithms Analysis**

We applied four machine learning algorithms, SVM-RFE, Lasso, Random Forest, and XGBoost, to further filter the independent prognostic genes. Genes identified by all four algorithms were selected for further analysis

**ROC Curve**

ROC curves were constructed to evaluate the predictive performance of the Support Vector Machine (SVM) algorithm, and multi-gene ROC curves were generated to assess the diagnostic sensitivity and specificity of the selected genes.

**Survival Curve Analysis**

We used TCGA tumor data and its clinical information as the test set to assess the prognostic impact of biomarker genes in GBM. Additionally, the GSE43378 and GSE83300 datasets were used as validation sets to further analyze the prognostic effect of these biomarkers in GBM. In R 4.4.0, the median expression value of each biomarker gene was used as the threshold to divide the samples into high and low expression groups, followed by survival analysis using the survival package.

**Single-gene Gene Set Enrichment Analysis (GSEA)**

We performed this analysis in R 4.4.0 using the GSEA package to further explore the relevant signaling pathways of these six biomarker genes. TCGA tumor expression data were used for this analysis. First, we calculated the correlation of each biomarker gene with all other genes and ranked them according to the log fold change (logFC) for subsequent analysis. Then, we downloaded the KEGG pathway dataset from the GSEA database (https://www.gsea-msigdb.org/gsea/index.jsp) as the standard for enrichment evaluation. The top 5 pathways from the final result were selected for display, and Table S1 lists the GSEA enrichment results for each biomarker gene.

**Table S1**

| Description | pvalue | p.adjust |
|---|---|---|
| REFERENCE_CYTOKINE_JAK_STAT_SIGNALING_PATHWAY | 7.222468053680833e-06 | 0.000123843639662769 |
| REFERENCE_TRANSLATION_INITIATION | 1.303617259608090e-05 | 0.000123843639662769 |
| REFERENCE_GENE_SILENCING_BY_METHYLATION_OF_H3K27_AND_UBIQUITINATION_OF_H2AK119 | 0.000486854527222385 | 0.003083412005741770 |
| REFERENCE_RAB7_REGULATED_MICROTUBULE_MINUS_END | 0.0061242092 | 0.02908999375 |

| | | |
|---|---|---|
| _DIRECTED_TRANSPORT | 1087074 | 1636 |
| REFERENCE_RETROGRADE_AXONAL_TRANSPORT | 0.012239008802119 4 | 0.046508233448053 7 |

DCTD

| Description | pvalue | p.adjust |
|---|---|---|
| REFERENCE_MITOCHONDRIAL_COMPLEX_UCP1_IN_THERMOGENESIS | 4.88480322895737e-08 | 1.17235277494977e-06 |
| VARIANT_MUTATION_CAUSED_ABERRANT_SNCA_TO_ELECTRON_TRANSFER_IN_COMPLEX_I | 8.78877103908839e-07 | 1.05465252469061e-05 |
| REFERENCE_CYTOKINE_JAK_STAT_SIGNALING_PATHWAY | 1.63053642055594e-06 | 1.30442913644475e-05 |
| REFERENCE_ELECTRON_TRANSFER_IN_COMPLEX_I | 2.99255711436612e-06 | 1.43642741489574e-05 |
| VARIANT_MUTATION_INACTIVATED_PINK1_TO_ELECTRON_TRANSFER_IN_COMPLEX_I | 2.99255711436612e-06 | 1.43642741489574e-05 |
| VARIANT_MUTATION_CAUSED_ABERRANT_TDP43_TO_ELECTRON_TRANSFER_IN_COMPLEX_I | 7.78072027704476e-06 | 3.11228811008179e-05 |
| VARIANT_MUTATION_CAUSED_ABERRANT_ABETA_TO_ELECTRON_TRANSFER_IN_COMPLEX_I | 1.12010680477625e-05 | 3.84036618708043e-05 |
| REFERENCE_WNT_SIGNALING_PATHWAY | 0.00135149244062096 | 0.00405447732186287 |
| VARIANT_FZD7_OVEREXPRESSION_TO_WNT_SIGNALING_PATHWAY | 0.00309268322786953 | 0.00824715527431873 |
| VARIANT_LRP6_OVEREXPRESSION_TO_WNT_SIGNALING_PATHWAY | 0.00519395826466617 | 0.01246549908351988 |
| VARIANT_MUTATION_CAUSED_ABERRANT_SNCA_TO_26S_PROTEASOME_MEDIATED_PROTEIN_DEGRADATION | 0.01327358500125638 | 0.02896054900118321 |

IL17RD

| Description | pvalue | p.adjust |
|---|---|---|
| REFERENCE_TRANSLATION_INITIATION | 6.48843638660036e-10 | 1.16791854958806e-08 |
| REFERENCE_CYTOKINE_JAK_STAT_SIGNALING_PATHWAY | 0.000113152207308795 | 0.00101836986577915 |
| REFERENCE_ITGA_B_RHOG_RAC_SIGNALING_PATHWAY | 0.00699791225797445 | 0.04198747354784677 |

TWSG1

| Description | pvalue | p.adjust |
|---|---|---|
| REFERENCE_TRANSLATION_INITIATION | 4.87894541583 89e-09 | 1.41489417059328e-07 |
| REFERENCE_CYTOKINE_JAK_STAT_SIGNALING_PATHWAY | 1.38936303748461e-08 | 2.01457640435268e-07 |
| REFERENCE_ITGA_B_TALIN_VINCULIN_SIGNALING_PATHWAY | 3.04372627177188e-07 | 2.94226872937948e-06 |
| REFERENCE_GENE_SILENCING_BY_METHYLATION_OF_H3K27_AND_UBIQUITINATION_OF_H2AK119 | 1.71049191493294e-06 | 1.24010663832638e-05 |
| REFERENCE_ITGA_B_RHOG_RAC_SIGNALING_PATHWAY | 0.000144690637617133 | 0.00083920569817937 4 |
| REFERENCE_ITGA_B_FAK_CDC42_SIGNALING_PATHWAY | 0.000207631752230362 | 0.00100355346911342 |
| REFERENCE_ITGA_B_FAK_RAC_SIGNALING_PATHWAY | 0.0002936815 | 0.0012166808 |

| | | |
|---|---|---|
| | 92462643 | 8305952 |
| REFERENCE_MITOCHONDRIAL_COMPLEX_UCP1_IN_THERMOGENESIS | 0.000634135412960826 | 0.002298740871198299 |
| REFERENCE_ADRB3_UCP1_SIGNALING_PATHWAY | 0.004379197916571874 | 0.014110748842309 3 |
| REFERENCE_TIGHT_JUNCTION_ACTIN_SIGNALING_PATHWAY | 0.013282505932136 5 | 0.038519267203195 8 |

OSMR

| Description | pvalue | p.adjust |
|---|---|---|
| REFERENCE_MITOCHONDRIAL_COMPLEX_UCP1_IN_THERMOGENESIS | 4.79757222056245e-25 | 1.19939305514061e-23 |
| REFERENCE_ELECTRON_TRANSFER_IN_COMPLEX_I | 6.69725030649 7e-16 | 5.581041922084e-15 |
| VARIANT_MUTATION_CAUSED_ABERRANT_SNCA_TO_ELECTRON_TRANSFER_IN_COMPLEX_I | 6.69725030649 7e-16 | 5.581041922084e-15 |
| VARIANT_MUTATION_INACTIVATED_PINK1_TO_ELECTRON_TRANSFER_IN_COMPLEX_I | 1.71251084733133e-15 | 1.07031927958208e-14 |
| VARIANT_MUTATION_CAUSED_ABERRANT_TDP43_TO_ELECTRON_TRANSFER_IN_COMPLEX_I | 3.37991978366445e-15 | 1.68995989183222e-14 |
| VARIANT_MUTATION_CAUSED_ABERRANT_ABETA_TO_ELECTRON_TRANSFER_IN_COMPLEX_I | 2.49860346858677e-14 | 1.04108477857782e-13 |
| VARIANT_MUTATION_CAUSED_ABERRANT_SOD1_TO_26S_PROTEASOME_MEDIATED_PROTEIN_DEGRADATION | 9.70974630021194e-05 | 0.000346776653578998 |
| REFERENCE_26S_PROTEASOME_MEDIATED_PROTEIN_DEGRADATION | 0.000298097441343685 | 0.000931554504199015 |
| REFERENCE_WNT_SIGNALING_PATHWAY | 0.000386523327648775 | 0.001073675901013549 |
| VARIANT_MUTATION_INACTIVATED_UBQLN2_TO_26S_PROTEASOME_MEDIATED_PROTEIN_DEGRADATION | 0.000495843238216389 | 0.001239608095554097 |
| VARIANT_MUTATION_INACTIVATED_VCP_TO_26S_PROTEASOME_MEDIATED_PROTEIN_DEGRADATION | 0.000917254212366556 | 0.002084668666446945 |
| VARIANT_MUTATION_CAUSED_ABERRANT_ABETA_TO_26S_PROTEASOME_MEDIATED_PROTEIN_DEGRADATION | 0.001507767 42193238 | 0.003141182129 02578 |
| REFERENCE_TRANSLATION_INITIATION | 0.001789140 18888924 | 0.003440654209 40239 |
| VARIANT_MUTATION_CAUSED_ABERRANT_HTT_TO_26S_PROTEASOME_MEDIATED_PROTEIN_DEGRADATION | 0.002827044 8508062 | 0.005048294376 43965 |
| REFERENCE_ADRB3_UCP1_SIGNALING_PATHWAY | 0.006577272 72334211 | 0.010962121205 5702 |
| REFERENCE_TRANSCRIPTION_COUPLED_NER | 0.016199794 5196434 | 0.025312178936 9428 |
| REFERENCE_RAB7_REGULATED_MICROTUBULE_MINUS_END_DIRECTED_TRANSPORT | 0.032035432 3814908 | 0.047110929972 7806 |

SEC11C

| Description | pvalue | p.adjust |
|---|---|---|
| REFERENCE_TRANSLATION_INITIATION | 5.16995682881154e-19 | 1.55098704864346e-17 |
| REFERENCE_PRE_IC_FORMATION | 1.94724667760 46e-07 | 2.92087001640 69e-06 |
| REFERENCE_CYTOKINE_JAK_STAT_SIGNALING_PATHWAY | 5.43404360693702e-06 | 5.43404360693702e-05 |

| | | |
|---|---|---|
| REFERENCE_ORIGIN_UNWINDING_AND_ELONGATION | 1.88856704130004e-05 | 0.000113314022478002 |
| REFERENCE_MITOCHONDRIAL_COMPLEX_UCP1_IN_THERMOGENESIS | 1.70732932834068e-05 | 0.000113314022478002 |
| VARIANT_MUTATION_CAUSED_ABERRANT_HTT_TO_26S_PROTEASOME_MEDIATED_PROTEIN_DEGRADATION | 4.58369227473168e-05 | 0.000196443954631358 |
| VARIANT_MUTATION_CAUSED_ABERRANT_SNCA_TO_26S_PROTEASOME_MEDIATED_PROTEIN_DEGRADATION | 4.58369227473168e-05 | 0.000196443954631358 |
| REFERENCE_26S_PROTEASOME_MEDIATED_PROTEIN_DEGRADATION | 8.56251709225857e-05 | 0.000256875512767757 |
| VARIANT_MUTATION_INACTIVATED_UBQLN2_TO_26S_PROTEASOME_MEDIATED_PROTEIN_DEGRADATION | 8.56251709225857e-05 | 0.000256875512767757 |
| VARIANT_MUTATION_INACTIVATED_VCP_TO_26S_PROTEASOME_MEDIATED_PROTEIN_DEGRADATION | 8.56251709225857e-05 | 0.000256875512767757 |
| VARIANT_MUTATION_CAUSED_ABERRANT_ABETA_TO_26S_PROTEASOME_MEDIATED_PROTEIN_DEGRADATION | 0.000467535029320387 | 0.00127509553451015 |
| VARIANT_MUTATION_CAUSED_ABERRANT_SOD1_TO_26S_PROTEASOME_MEDIATED_PROTEIN_DEGRADATION | 0.000726063305346474 | 0.001815158 26336619 |
| REFERENCE_ITGA_B_TALIN_VINCULIN_SIGNALING_PATHWAY | 0.001104714 76371169 | 0.002549341 76241159 |
| VARIANT_SCRAPIE_CONFORMATION_PRPSC_TO_26S_PROTEASOME_MEDIATED_PROTEIN_DEGRADATION | 0.001593370 17005588 | 0.003414364 65011974 |
| REFERENCE_GENE_SILENCING_BY_METHYLATION_OF_H3K27_AND_UBIQUITINATION_OF_H2AK119 | 0.002404204 31727433 | 0.004808408 63454865 |
| REFERENCE_ELECTRON_TRANSFER_IN_COMPLEX_I | 0.019519979 13022 | 0.032533298 5503666 |
| VARIANT_MUTATION_CAUSED_ABERRANT_SNCA_TO_ELECTRON_TRANSFER_IN_COMPLEX_I | 0.019519979 13022 | 0.032533298 5503666 |
| VARIANT_MUTATION_CAUSED_ABERRANT_TDP43_TO_ELECTRON_TRANSFER_IN_COMPLEX_I | 0.019519979 13022 | 0.032533298 5503666 |

SMARCB1

**Single-gene Gene Set Variation Analysis (GSVA)**

We conducted this analysis in R 4.4.0 using the GSVA package, a method for analyzing gene set variation. First, we downloaded the classic 50 KEGG cancer signaling pathway datasets from the GSEA database (https://www.gsea-msigdb.org/gsea/index.jsp) as the standard for enrichment analysis. Then, in the GBM data, we divided the samples into high and low expression groups based on the median expression value of each biomarker gene and performed differential analysis using the limma package. Pathways with t-values greater than 0 and p-values less than 0.05 were categorized as upregulated, while pathways with t-values less than 0 and p-values less than 0.05 were categorized as downregulated.

**Differential Analysis of GSVA-Enriched Pathways and Correlation with Marker Genes**

To further explore potential signaling pathways regulating biomarker genes, we used the limma package in R 4.4.0 to analyze differential signaling pathways between GBM and normal samples in the merged TCGA and GTEx data. We also analyzed the correlation between these differential signaling pathways and the biomarker genes. First, we set the threshold for significant differential signaling pathways as $|\log FC| = 2$ and $p < 0.05$. We then analyzed the correlation between each biomarker gene and these significant differential signaling pathways, as well

as the correlation between the pathways themselves.

**Drug Prediction and ceRNA Network Construction**

We used the DSigDB database (https://dsigdb.tanlab.org/DSigDBv1.0/) to predict the target drugs for these biomarker genes. Additionally, we constructed the mRNA-miRNA interaction network for these biomarker genes using the miRDB database (https://mirdb.org/) and the TargetScan database (https://www.targetscan.org/vert_80/). We also built the miRNA-lncRNA interaction network using the starBase database (https://rnasysu.com/encori/index.php). These target drug networks and ceRNA networks for the biomarker genes were visualized using Cytoscape software.

**Marker Genes Expression Analysis**

We used the merged TCGA and GTEx data as the test set, and the GSE4290 dataset as the validation set, to analyze the differential expression of each biomarker gene between GBM and normal samples.

**Clinical Samples Acquisition**

The clinical samples used to validate biomarker gene expression were obtained from two GBM samples and two adjacent tumor tissues surgically resected by the Neurosurgery Department at Qingdao University Affiliated Hospital. This study was approved by the Ethics Committee of Qingdao University Affiliated Hospital.

**Fluorogenic Quantitative PCR Analysis**

Total RNA from clinical samples was extracted using the TRNzol Total RNA Extraction Reagent Kit (TianGen Biotech, Beijing). The forward and reverse primers for these biomarker genes are listed as follows: “h-DCTD-F TTGCCTTG GAGAAGGACAGCAG”, “h-DC D-R ACT ACAGCCTTTCACATCGGTCG”, “h-SEC11C-F GGCTGGAAAA GAAGGACGT GGT”,“h-SEC 11C-R GCACCCATTACAG CCAAAAGAGC”, “h-OSMR-F CAGGTGTTCC TACCAAATCT GCG”, “h-OSMR-RAATCCACCCTCTGT GC CTGCAA”, “h-SMARCB1-F GGCATCAGAAG ACCTACGCCTT”, “h-SMARCB1-R CTCCATC TCAGCGTCTGTC AGA”, “h-TWSG1-F CTT TGGGACGAGTGCTGTGACT”, “h-TWSG1-R GAGAAGGGATCGGTTCATGCAG”, “h-IL1 7RD-F GAATGTCGTCCAGTGTTTCGCC”, “h-IL17RD-R GATGAACTGGGACTCGTGGAT C ”, “h-GAPDH-F GACCTGACCTGCCGTCTA”, and “h-GAPDH-R AGGAGTGGGTGTCGCTGT ”, which is listed in Table S2. mRNA reverse transcription was performed using the cDNA Synthesis Kit (TaKaRa, RR047A), and the resulting cDNA was stored at -20°C for later use. Quantitative PCR was then performed using the Quantitative PCR Kit (TaKaRa, RR820A). The cDNA samples were diluted 10-fold and used as templates for PCR detection (ABI 7500 Fluorescent Quantitative PCR Instrument). The data were saved, and GAPDH was used as the internal control for relative quantification. Statistical analysis was performed using the T-test in GraphPad.

**Table S2**

| Gene Name | Primer Seqence | Length |
|---|---|---|
| h-DCTD-F | TTGCCTTGGAGAAGGACAGCAG | 132 |
| h-DCTD-R | ACTACAGCCTTTCACATCGGTCG | |
| h-SEC11C-F | GGCTGGAAAAGAAGGACGTGGT | 157 |
| h-SEC11C-R | GCACCCATTACAGCCAAAAGAGC | |
| h-OSMR-F | CAGGTGTTCCTACCAAATCTGCG | 144 |

| | | |
|---|---|---|
| h-OSMR-R | AATCCACCCTCTGTGCCTGCAA | |
| h-SMARCB1-F | GGCATCAGAAGACCTACGCCTT | 116 |
| h-SMARCB1-R | CTCCATCTCAGCGTCTGTCAGA | |
| h-TWSG1-F | CTTTGGGACGAGTGCTGTGACT | 163 |
| h-TWSG1-R | GAGAAGGGATCGGTTCATGCAG | |
| h-IL17RD-F | GAATGTCGTCCAGTGTTTCGCC | 119 |
| h-IL17RD-R | GATGAACTGGGACTCGTGGATC | |
| h-GAPDH-F | GACCTGACCTGCCGTCTA | 83 |
| h-GAPDH-R | AGGAGTGGGTGTCGCTGT | |

## Discussion

GBM is one of the most aggressive intracranial tumors, and the current standard treatment remains surgery combined with radiotherapy and chemotherapy(Barbosa et al., 2014; Yi et al., 2019). However, due to the unique location of GBM in the human body and the blood-brain barrier's blocking effect on most small-molecule drugs, the median survival rate for GBM patients is only around 14 months, with a 5-year survival rate of 4-5%(B. Huang et al., 2021; Lu et al., 2022). Therefore, it is crucial to find more effective treatments for GBM and explore diagnostic biomarkers for this disease. Increasing evidence shows that there are multiple biomarkers in GBM that play an important role in its treatment. One study revealed that TRIM7 is highly expressed in GBM and promotes tumor progression. However, silencing TRIM7 can increase GBM sensitivity to temozolomide by regulating NCOA4-mediated ferroptosis(Li et al., 2022). Another study showed that LGALS3 promotes GBM resistance to ionizing radiation and temozolomide, and it is an independent prognostic factor for GBM patients. It may be a marker gene to improve therapeutic resistance and increase patient survival(Wang et al., 2019). Therefore, further identification of marker genes related to the pathogenesis of GBM and investigation of their prognostic value may provide novel targeted therapeutic directions for clinical treatment.

Using bioinformatics methods to screen disease-specific genes and explore molecular mechanisms related to the disease is an effective research approach. This method not only allows for the observation of general regulatory mechanisms in disease progression but also provides clear research directions for subsequent molecular experiments. In this study, we combined bioinformatics and machine learning to investigate the mechanisms of disulfidptosis - related genes in GBM. Our results suggest that six marker genes, including DCTD, IL17RD, SMARCB1, TWSG1, OSMR, and SEC11C, are of significant potential prognostic value for GBM patients. Through Gene Set Enrichment Analysis (GSEA) and Gene Set Variation Analysis (GSVA), we found that these genes are closely associated with multiple tumor-related signaling pathways, including the IL6_JAK_STAT3, P53, PI3K_AKT, and KRAS signaling pathways. Interestingly, except for SEC11C, the genes DCTD, TWSG1, OSMR, SMARCB1, and IL17RD are significantly enriched in the JAK_STAT3 signaling pathway, and differential analysis showed that the JAK_STAT3 signaling pathway is also significantly different between GBM and normal tissues. As we all know, the STAT protein family includes STAT1, STAT2,

STAT3, STAT4, STAT5A, STAT5B, and STAT6(S. J. Liu, Dang, Lim, Feng, & Maher, 2021). Among these, STAT3 has the most characteristic oncogenic activity(H. Liu & Tang, 2023). Abnormal expression of STAT3 can promote angiogenesis, immune evasion, and apoptosis resistance in GBM by regulating the transcription of related genes. These signaling targets mainly include Bcl-xL, Bcl-2, cyclin D1, and c-Myc(H. Huang, Weng, & Chen, 2020). Moreover, numerous studies have shown that the STAT3 signaling pathway is involved in regulating GBM drug resistance. For example, activation of the STAT3 pathway can promote TMZ resistance in tumor cells by inhibiting the degradation of MGMT in GBM cells(Jia et al., 2016). Additionally, studies have shown that PIKE-A can activate the phosphorylation level of STAT3, suppressing the transcriptional activity of 6-phosphogluconate dehydrogenase and leading to tumor cell metabolic reprogramming, ultimately contributing to TMZ resistance(He et al., 2020). This provides direction for our subsequent research.

We then validated the expression of these marker genes in GBM using the GSE43378, GSE4290, and GSE83300 datasets and performed survival analysis. Finally, we validated the expression of these genes through quantitative real-time PCR, and the results were consistent with the trends observed in the TCGA dataset and validation datasets. These findings suggest that these six marker genes may potentially regulate the progression and drug resistance of GBM through the JAK-STAT3 signaling pathway and have reliable clinical research value.

However, there are some limitations in this study. First, the relatively small sample size of the datasets used may affect the generalizability of the results. Second, this study mainly utilized bioinformatics methods, and only quantitative real-time PCR was used for experimental validation. There is a lack of further validation through various in vitro and in vivo experiments, which reduces the reliability of the study. Moreover, this study only explored biomarkers for GBM and did not further investigate the specific signaling pathways and biological processes these biomarkers are involved in. These are the limitations of this study. To address these shortcomings, future research should focus on the following aspects: First, conduct various in vitro experiments to validate the specific biological functions of these marker genes, delving into the specific signaling pathways and drug resistance mechanisms in GBM. Second, validate the roles of these marker genes in animal models to provide new potential targeted therapeutic directions for the clinical treatment of GBM.

## Conclusion

In conclusion, this study provides new insights into the molecular mechanisms of potential diagnostic biomarkers for GBM, including the diagnostic and prognostic efficacy of these marker genes in GBM, especially the potential value of signaling pathways (such as the JAK-STAT3 pathway) that these marker genes may be involved in, in the development, progression, and drug resistance of GBM. The ceRNA network of these marker genes and the prediction network for targeted drugs offer new directions for targeted therapy in GBM, providing fresh perspectives for clinical treatment. For future research, we should prioritize the validation of the specific biological functions of these marker genes, elucidating the specific signaling pathways they are involved in and evaluating the efficacy of targeted therapies, and providing potential therapeutic targets for clinical treatment.

## Statements and Declarations

## Acknowledgements

We greatly appreciate all the contributors and researchers who have organized and publicly made available the TCGA, UCSC Xena, and GEO datasets. We are very grateful to the

Chinese Postdoctoral Science Foundation (grant no. 2021M691696) very much for providing us with funding. We would also like to extend our sincere gratitude to all the researchers who contributed to this study.

**Funding**

This research was supported by the China Postdoctoral Science Foundation funded project (grant no. 2021M691696).

**Competing Interests**

The authors have no relevant financial or non-financial interests to disclose.

**Author Contributions**

All authors contributed to the study. Conceptualization, Visualization and Writing-original draft were performed by Daikang Xu; Formal Analysis and Methodology were performed by Guangyu Du; Data Curation and Software were achieved by Jingxian Sun; Resources and Validation were finished by Xiaolei Lan and Zhiyong Yan; Project Administration and Supervision were achieved by Jianpeng Wang.

**Data Availability**

The datasets analysed during the current study are available from the TCGA database (https://portal.gdc.cancer.gov/), GEO database (https://www.ncbi.nlm.nih.gov/geo/), and GTEx database (https://portal.gdc.cancer.gov/). Data from the analysis can be obtained from the corresponding author upon reasonable request.

**Ethics Declarations**

This study was performed in line with the principles of the Declaration of Helsinki. Approval was granted by the Ethics Committee of Affiliated hospital of Qingdao University (Date May 8th, 2025; Approval number QYFYWZ LL30036).

**References**

1. Barbosa, B. J. A. P., Mariano, E. D., Batista, C. M., Marie, S. K. N., Teixeira, M. J., Pereira, C. U., . . . Lepski, G. A. (2014). Intraoperative assistive technologies and extent of resection in glioma surgery: a systematic review of prospective controlled studies. *Neurosurgical Review, 38*(2), 217-227. doi:10.1007/s10143-014-0592-0
2. Goji, T., Takahara, K., Negishi, M., & Katoh, H. (2017). Cystine uptake through the cystine/glutamate antiporter xCT triggers glioblastoma cell death under glucose deprivation. *Journal of Biological Chemistry, 292*(48),19721-19732. doi:10.1074/jbc.M117.814392
3. He, X., Sheng, J., Yu, W., Wang, K., Zhu, S., & Liu, Q. (2020). LncRNA MIR155HG Promotes Temozolomide Resistance by Activating the Wnt/β-Catenin Pathway Via Binding to PTBP1 in Glioma. *Cellular and Molecular Neurobiology, 41*(6), 1271-1284. doi:10.1007/s10571-020-00898-z
4. Huang, B., Li, X., Li, Y., Zhang, J., Zong, Z., & Zhang, H. (2021). Current Immunotherapies for Glioblastoma Multiforme. *Frontiers in Immunology, 11*. doi:10.3389/fimmu.2020.603911
5. Huang, H., Weng, H., & Chen, J. (2020). m6A Modification in Coding and Non-coding RNAs: Roles and Therapeutic Implications in Cancer. *Cancer Cell, 37*(3), 270-288. doi:10.1016/j.ccell.2020.02.004
6. Jia, X., Wang, Z., Qiu, L., Yang, Y., Wang, Y., Chen, Z., . . . Yu, L. (2016). Upregulation of LncRNA-HIT promotes migration and invasion of non-small cell lung cancer cells by association with ZEB1. *Cancer Medicine, 5*(12), 3555-3563. doi:10.1002/cam4.948
7. Joly, J. H., Delfarah, A., Phung, P. S., Parrish, S., & Graham, N. A. (2020). A synthetic lethal drug combination mimics glucose deprivation–induced cancer cell death in the

presence of glucose. *Journal of Biological Chemistry, 295*(5),1350-1365. doi:10.1016/s 0021-9258(17)49891-7

8. Lee, S., Weiss, T., Bühler, M., Mena, J., Lottenbach, Z., Wegmann, R., . . . Snijder, B. (2024). High-throughput identification of repurposable neuroactive drugs with potent anti-glioblastoma activity. *Nature Medicine, 30*(11), 3196-3208. doi:10.1038/s41591-024-03224-y
9. Li, K., Chen, B., Xu, A., Shen, J., Li, K., Hao, K., . . . Wang, Z. (2022). TRIM7 modulates NCOA4-mediated ferritinophagy and ferroptosis in glioblastoma cells. *Redox Biology, 56*. doi:10.1016/j.redox.2022.102451
10. Liu, H., & Tang, T. (2023). Pan-cancer genetic analysis of disulfidptosis-related gene set. *Cancer Genet, 278-279*,91-103. doi:10.10 16/j.cancergen.2023.10.001
11. Liu, S. J., Dang, H. X., Lim, D. A., Feng, F. Y., & Maher, C. A. (2021). Long noncoding RNAs in cancer metastasis. *Nature Reviews Cancer, 21*(7), 446-460. doi:10.1038/s41568-021-00353-1
12. Liu, X., Nie, L., Zhang, Y., Yan, Y., Wang, C., Colic, M., . . . Gan, B. (2023). Actin cytoskeleton vulnerability to disulfide stress mediates disulfidptosis. *Nature Cell Biology, 25*(3), 404-414. doi:10.1038/s41556-023-010 91-2
13. Lu, G., Wang, X., Li, F., Wang, S., Zhao, J., Wang, J., . . . Wei, W. (2022). Engineered biomimetic nanoparticles achieve targeted delivery and efficient metabolism-based synergistic therapy against glioblastoma. *Nature Communications, 13*(1). doi:10.1038/ s41467-022-31799-y
14. Ma, Q., Jiang, H., Ma, L., Zhao, G., Xu, Q., Guo, D., . . . Lu, Z. (2023). The moonlighting function of glycolytic enzyme enolase-1 promotes choline phospholipid metabolism and tumor cell proliferation. *120*(15), e2209 435120. doi:doi:10.1073/pnas.2209435120
15. Mandal, M., Banerjee, I., & Mandal, M. (2025). Effective approaches in conquering chemoresistance of glioblastoma: potential for nanoformulations. *Drug Delivery and Translational Research*. doi:10.1007/s13346-025-01859-z
16. Qin, A., Musket, A., Hilton, B., Preiszner, J., Krenciute, G., Berens, M. E., . . . Xie, Q. (2025). Efficacy of MET-targeting CAR T cells against glioblastoma patient-derived xenograft models. *Journal of Translational Medicine, 23*(1). doi:10.1186/s12967-025-064 75-6
17. Rodríguez-Camacho, A., Flores-Vázquez, J. G., Moscardini-Martelli, J., Torres-Ríos, J. A., Olmos-Guzmán, A., Ortiz-Arce, C. S., . . . Moreno-Jiménez, S. (2022). Glioblastoma Treatment: State-of-the-Art and Future Perspectives. *International Journal of Molecular Sciences, 23*(13). doi:10.3390/ ijms 23137207
18. Tamai, S., Ichinose, T., Tsutsui, T., Tanaka, S., Garaeva, F., Sabit, H., & Nakada, M. (2022). Tumor Microenvironment in Glioma Invasion. *Brain Sciences, 12*(4). doi:10.3390/ brainsci1 2040505
19. Tummers, B., & Green, D. R. (2017). Caspase-8: regulating life and death. *Immunological Reviews, 277*(1),76-89. doi: 1 0.1111/imr.12541
20. Wang, H., Song, X., Huang, Q., Xu, T., Yun, D., Wang, Y., . . . Chen, J. (2019). LGALS3 Promotes Treatment Resistance in Glioblastoma and Is Associated with Tumor Risk and Prognosis. *Cancer Epidemiology, Biomarkers & Prevention, 28*(4), 760-769. doi:10.1158/1055-9965.Epi-18-0638
21. Xu, J., Guo, Y., Ning, W., Wang, J., Chen, Y., Liu, D., . . . Zhang, H. (2025). Comprehensive analysis of heat shock proteins in glioma revealed the association with glioma-associated myeloid cells. *Genes & Immunity*. doi:10.1038/s41435-025-00327-5
22. Yi, H. G., Jeong, Y. H., Kim, Y., Choi, Y. J., Moon, H. E., Park, S. H., . . . Cho, D. W.

(2019). A bioprinted human-glioblastoma-on-a-chip for the identification of patient-specific responses to chemoradiotherapy. *Nat Biomed Eng, 3*(7), 509-519. doi:10.1038/s41551-019-0363-x

23. Zhang, S., Wang, Y., Sun, B., Zhu, S., Jia, Z., Liu, L., & Liu, L. (2025). Regulation of Glycolysis by SMAD5 in Glioma Cells: Implications for Tumor Growth and Apoptosis. *Neurochemical Research, 50*(2). doi:10.1007/s11064-025-04352-8
24. Zhao, G., Zhao, Z., Xia, M., Xiao, L., Zhu, B., Wang, H., . . . Di, J. (2023). CPEB2 inhibit cell proliferation through upregulating p21 mRNA stability in glioma. *Scientific Reports, 13*(1). doi:10.1038/s41598-023-50848-0